Electronic Supplementary Material (ESI) for Journal of Materials Chemistry C.

Supplementary information

A comparison of *para*, *meta*, and *ortho*-carborane centred non-fullerene acceptors for organic photovoltaics

Filip Aniés,[a] Francesco Furlan,[a] Zhuoran Qiao,[a] Valentina Pirela,[b] Matthew Bidwell,[a] Martina Rimmele,[a] Jaime Martín,[b,c,d] Nicola Gasparini,[a] Martin Heeney[a,e]*

[a] Department of Chemistry and Centre for Processable Electronics, Imperial College London, Molecular Sciences Research Hub, 80 Wood Lane, London, W12 0BZ, UK

[b] POLYMAT, University of the Basque Country UPV/EHU Av. de Tolosa 72, Donostia-San Sebastián, Spain

[c] Universidade da Coruña, Grupo de Polímeros, Centro de Investigacións Tecnolóxicas (CIT), Esteiro, 15471 Ferrol, Spain

[d]Ikerbasque, Basque Foundation for Science, 48013 Bilbao, Spain

[e] KAUST Solar Center (KSC), Physical Science and Engineering Division (PSE), King Abdullah University of Science and Technology (KAUST), Thuwal, 23955-6900, Saudi Arabia

Characterisation

AFM images of spin coated films (10 mg/mL solutions in chlorobenzene, 1000 rpm for 1 min) were obtained with an Agilent AFM 5500 setup in tapping mode, and processed with the PicoView 1.5 software.

TGA was run on a Mettler Toledo TGA/DSC 1 from 50 to 750 °C at 5 °C/min under nitrogen.

UV-vis absorption was measured on a Cary 60 UV-Vis Spectrophotometer, and PL on a Cary Eclipse Fluorescence Spectrometer (λ_{ex} = 375 nm).

CV was performed using an Autolab PGSTAT101 potentiostat: the sample was drop-cast onto a glassy carbon working electrode, and measured at 0.1 V/s using a Pt counter electrode and a Ag/Ag^+ reference electrode, all submerged in a 0.1 M solution of tetrabutylammonium hexafluorophosphate in acetonitrile. Ferrocene was added at the end of the measurements to provide an internal reference.

Computational models of each NFA compound, with methyl groups in place of alkyl chains for the sake of computational feasibility, were optimised with Gaussian 16 on the B3LYP/6-311G** level.[S1,S2] Molecular structures and orbitals were visualised in GaussView 5.0. Time-dependent DFT was computed on the 6-311G** level with 20 N-states.

GIWAXS measurements were performed at the BL11 NCD-SWEET at ALBA Synchrotron Radiation Facility (Barcelona, Spain). The incident X-ray beam energy was set to 12.4 eV using a channel cut Si (1 1 1) monochromator. The angle of incidence α_i was set between 0.1º and 0.2º to ensure surface sensitivity. Data are expressed as a function of the scattering vector, which was calibrated using Cr_2O_3, obtaining a sample-to-detector distance of 145.6 mm. The scattering patterns were recorded using a Rayonix LX255-HS area detector, which consists of a pixel array of 1920 × 5760 pixels (H × V) with a pixel size of 44 × 44 μm^2. All the measurements were performed under N_2 atmosphere to minimize the damage of the films. 2D GIWAXS patterns were corrected as a function of the components of the scattering vector (q).

OPV fabrication

All devices are fabricated with an inverted structure configuration (ITO/ZnO/Active layer/MoO_3/Ag). Pre-patterned indium tin oxide (15 Ω sq^{-1}) substrates were cleaned by sonication in detergent, deionized water, acetone and isopropanol followed by oxygen plasma treatment for 7 min. A 40 nm ZnO layer was deposited onto the substrate by spin coating at 4000 rpm for 40 s using a ZnO colloidal solution (219 mg zinc acetate dihydrate precursor in 60.4 µL 1-ethanolamine and 2 ml 2-methoxyethanol), followed by annealing at 180 °C for 15 min. Active layer solutions were prepared by dissolving donor polymer PBDB-T with each acceptor NFA described herein in a 1:1 ratio (wt/wt) at 20 mg/mL in chlorobenzene. Prior deposition, all solutions are heated up at 40°C for 1h. All active layers are deposited at a spin speed of 2000 rpm for 40 s. After annealing, 10 nm MoO_3 and 100 nm Ag layers were sequentially deposited onto the substrates via thermal evaporation, at 0.15 Å s^{-1} and 0.5 Å s^{-1} - 1 Å s^{-1} respectively. Each device featured 6 pixels with an area of 0.045 cm^2. Current density-Voltage (J–V) measurements were conducted using a filtered 300W xenon lamp (Oriel Instruments) for AM 1.5 G solar illumination of 100 mW/cm^2, calibrated with a standard Silicon photodiode, and a Keithley 2400 source meter ranging from -0.2 V to 1 V and corrected for spectral mismatch.

SCLC fabrication

Hole-only and electron-only SCLC devices were fabricated onto patterned ITO glass, following the above cleaning protocol. Hole-only and electron-only devices were fabricated with the structures ITO/PEDOT:PSS/blend/Au and ITO/ZnO/PEIE/blend/Ca/Al, respectively. PEDOT:PSS (Al4083) was spin coated to obtain a layer with a thickness of 40nm. ZnO was prepared and applied as outlined above, followed by rinsing with PEIE diluted at 0.5 wt% in 2-Methoxyethanol. All active layer blends were deposited according to OPV procedures. Active layer thicknesses were measured using a Dektak profilometer and all J-V curves were recorded with a Keithley 2400.

To extrapolate mobility values the Murgatroyd equation was employed:

$$J = \frac{9}{8}\mu_0 \varepsilon \frac{V^2}{d^3} exp\left(0.89\gamma \sqrt{\frac{V}{d}}\right)$$

where ε is the relative dielectric constant of the material (3 was assumed), ε_0 is the vacuum permittivity, μ is the mobility, *d* is the film thickness, γ is the field activation factor of mobility, and *V* is the applied voltage. When extracting the values of μ_0 and γ from the experimental data, the value of μ at any field *E* can be obtained by using the Poole–Frenkel expression:

$$\mu = \mu_0 exp(\gamma\sqrt{E})$$

Figures and tables

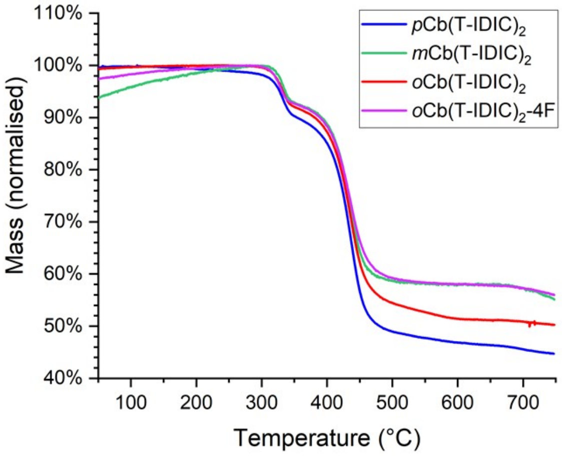

Figure S1. Thermogravimetric analysis highlighting decomposition temperatures of the featured NFAs.

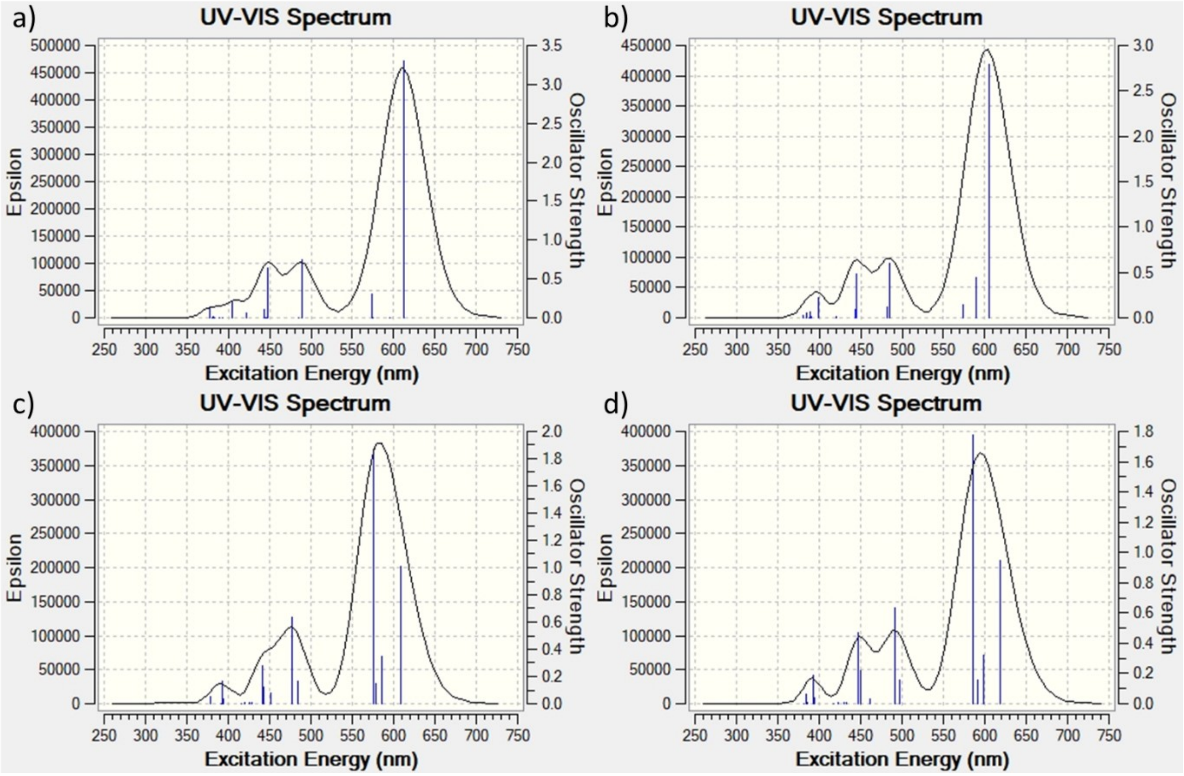

Figure S2. TD-DFT simulated absorption spectra of a) *p*Cb(T-IDIC)$_2$, b) *m*Cb(T-IDIC)$_2$, c) *o*Cb(T-IDIC)$_2$, and d) *o*Cb(T-IDIC)$_2$-4F.

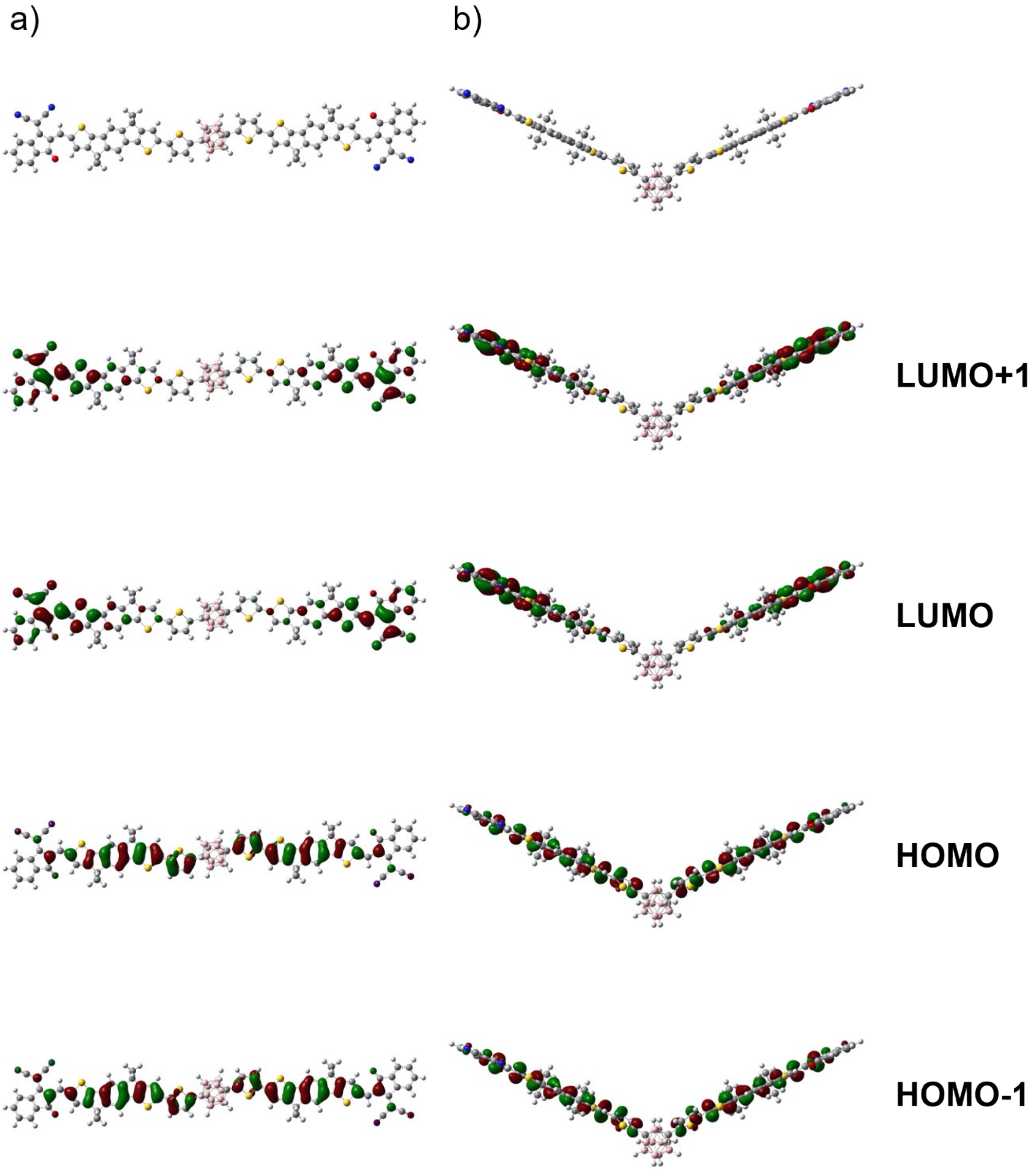

Figure S3. DFT optimised molecular structures and MOs of a) *p*Cb(T-IDIC)$_2$, b) *m*Cb(T-IDIC)$_2$, c) *o*Cb(T-IDIC)$_2$, and d) *o*Cb(T-IDIC)$_2$-4F.

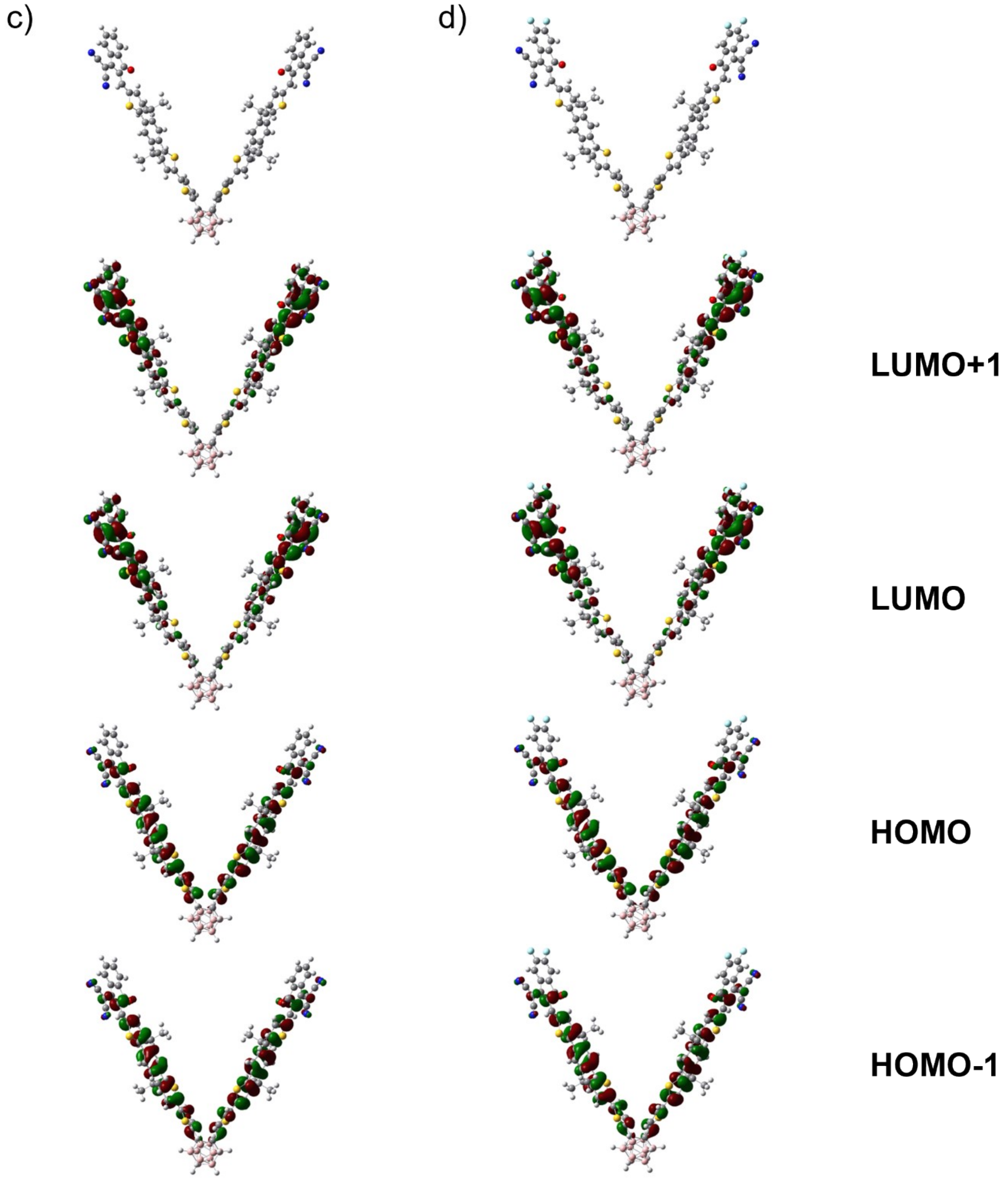

Figure S3. Continued.

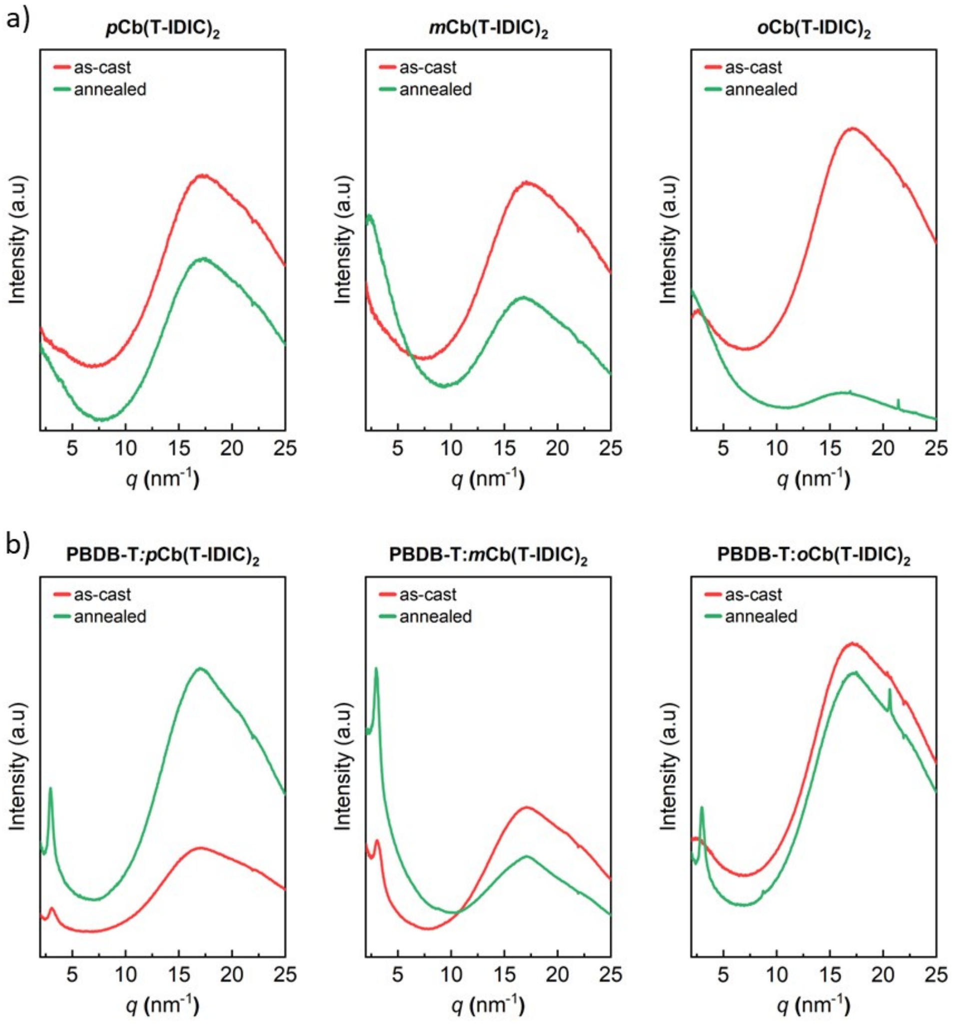

Figure S4. GIWAXS diffractograms (combined directional planes) of a) pristine and polymer blend films, before and after annealing.

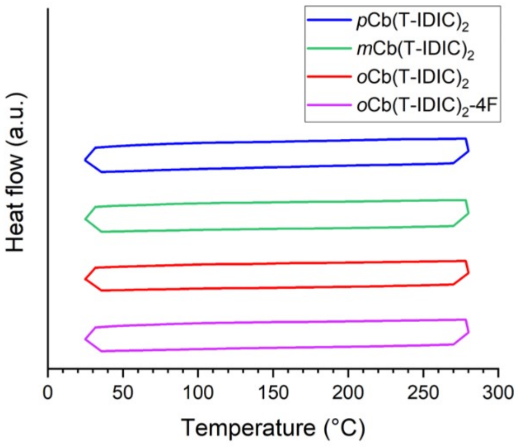

Figure S5. DSC scans of the featured NFAs.

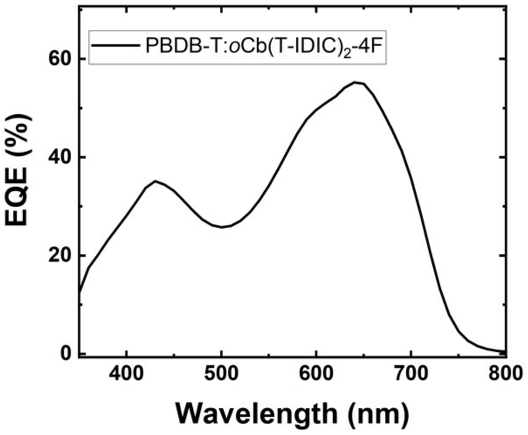

Figure S6. EQE of an OPV device employing *o*Cb(T-IDIC)$_2$-4F as the NFA.

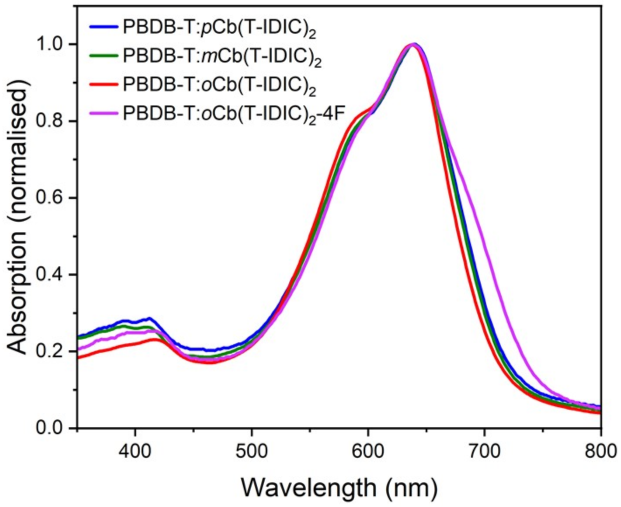

Figure S7. Absorption spectra of thin films of PBDB-T:NFA blends.

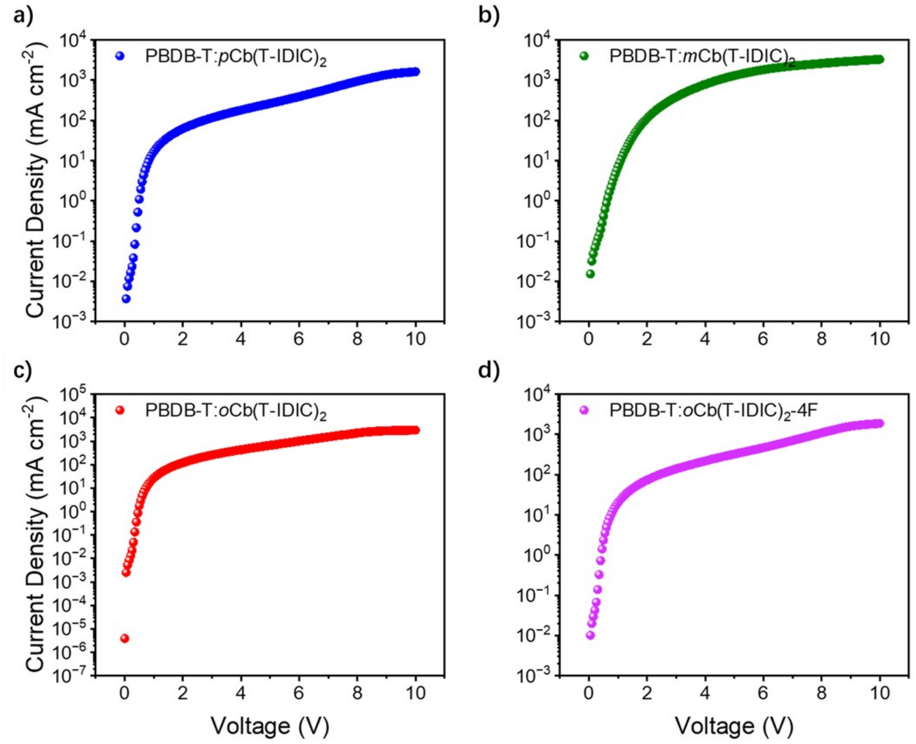

Figure S8. J-V characteristics of hole-only SCLC devices made with blends of PBDB-T and a) *p*Cb(T-IDIC)$_2$, b) *m*Cb(T-IDIC)$_2$, c) *o*Cb(T-IDIC)$_2$, and d) *o*Cb(T-IDIC)$_2$-4F. Active layer thicknesses were 90 nm, except for *m*Cb(T-IDIC)$_2$ at 80 nm.

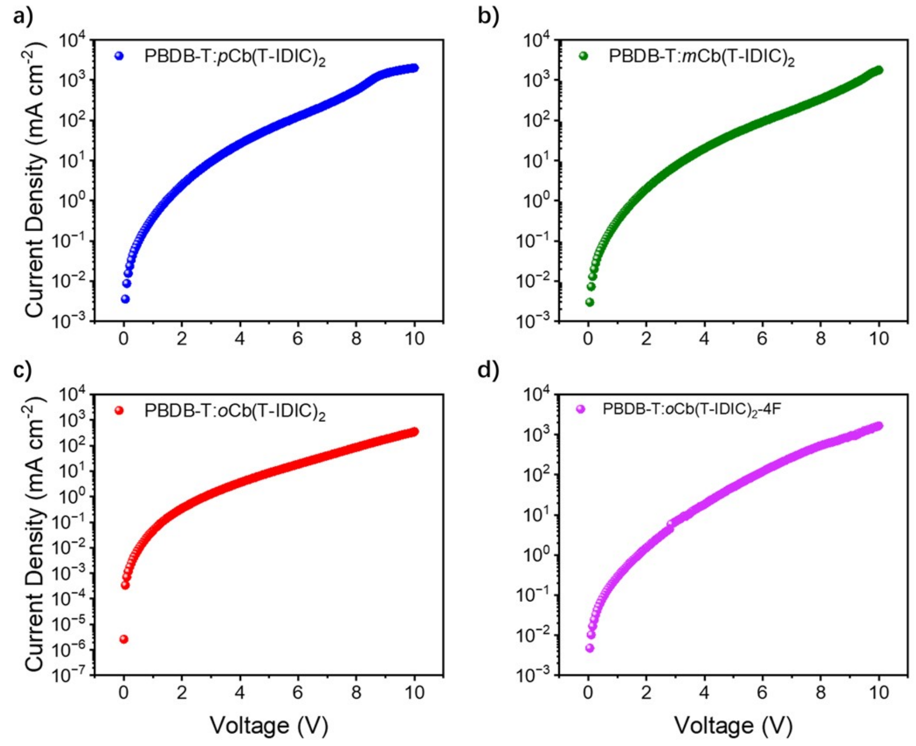

Figure S9. J-V characteristics of electron-only SCLC devices made with blends of PBDB-T and a) *p*Cb(T-IDIC)$_2$, b) *m*Cb(T-IDIC)$_2$, c) *o*Cb(T-IDIC)$_2$, and d) *o*Cb(T-IDIC)$_2$-4F. Active layer thicknesses were 90 nm, except for *m*Cb(T-IDIC)$_2$ at 80 nm.

Material	**μ_h (cm^2 V^{-1} s^{-1})**	**μ_e (cm^2 V^{-1} s^{-1})**	**μ_e/μ_h**
PBDB-T	1.51×10^{-5}	-	-
PBDB-T:*p*Cb(T-IDIC)$_2$	3.46×10^{-5}	1.85×10^{-7}	5.33×10^{-3}
PBDB-T:*m*Cb(T-IDIC)$_2$	6.07×10^{-5}	1.26×10^{-7}	2.08×10^{-3}
PBDB-T:*o*Cb(T-IDIC)$_2$	2.72×10^{-5}	1.74×10^{-7}	6.39×10^{-3}
PBDB-T:*o*Cb(T-IDIC)$_2$-4F	2.78×10^{-5}	6.04×10^{-7}	2.17×10^{-2}

Table S1. Hole and electron mobilities as derived from SCLC data, and corresponding μ_e/μ_h ratios of each blend.

Synthesis

General:

Chemicals were obtained from commercial sources and used without further purification, unless otherwise specified. Recycling preparative GPC was performed with a LaboACE LC-5060 equipped with Jaigel 2HR and 2.5HR columns, 20 mm ID × 600 mm each. Microwave reactions were run in a Biotage Initiator+ microwave reactor.

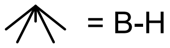

4,4,9,9-tetraoctyl-4,9-dihydro-*s*-indaceno[1,2-*b*:5,6-*b′*]dithiophene-2-carbaldehyde (2):

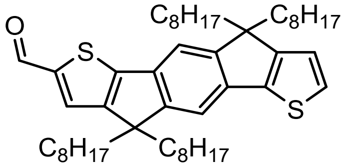

To a solution of 4,4,9,9-tetraoctyl-4,9-dihydro-*s*-indaceno[1,2-*b*:5,6-*b′*]dithiophene (2.028 g, 2.84 mmol, 1 eq.) in ice-cold degassed anhydrous DMF (80 mL) under nitrogen was added phosphorous oxychloride (0.28 mL, 2.99 mmol, 1.06 eq.), and the mixture was heated to 50 °C and left stirring overnight. To the solution was added saturated sodium acetate (50 mL), followed by stirring for 30 min. The crude product was extracted into dichloromethane (3 × 50 mL), and the combined organic layer was washed with 100 mL deionised water and 100 mL brine, and dried over Na_2SO_4. The product was isolated by column chromatography using dichloromethane and petroleum ether (v/v = 1:1) to afford 1.674 g orange crystalline solids (79 % yield):

^{1}H NMR (400 MHz, Chloroform-*d*) δ 9.88 (s, 1H), 7.62 (s, 1H), 7.40 (s, 1H), 7.34 (d, *J* = 4.8 Hz, 1H), 7.31 (s, 1H), 6.98 (d, *J* = 4.8 Hz, 1H), 2.08 – 1.94 (m, 4H), 1.93 – 1.81 (m, 4H), 1.27 – 1.02 (m, 48H), 0.81 (td, *J* = 7.0, 1.3 Hz, 12H).

^{13}C NMR (101 MHz, Chloroform-*d*) δ 184.79, 156.64, 155.12, 154.05, 152.88, 143.28, 141.21, 138.65, 133.86, 130.72, 127.92, 121.95, 115.04, 113.33, 54.17, 53.98, 39.17, 31.93, 30.07, 29.42, 29.34, 24.39, 24.30, 22.74, 14.21.

7-bromo-4,4,9,9-tetraoctyl-4,9-dihydro-*s*-indaceno[1,2-*b*:5,6-*b′*]dithiophene-2-carbaldehyde (3):

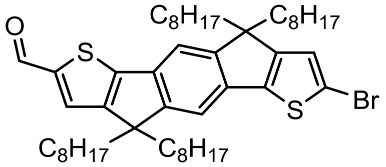

To a solution of 4,4,9,9-tetraoctyl-4,9-dihydro-*s*-indaceno[1,2-*b*:5,6-*b′*]dithiophene-2-carbaldehyde (1.674 g, 2.25 mmol, 1 eq.) in ice-cold THF (100 mL) under nitrogen was added N-bromosuccinimide (447 mg, 2.51 mmol, 1.1 eq.). After warming to room temperature and stirring overnight, the solution was added to deionised water (100 mL) and extracted into ethyl acetate (3 × 50 mL). The combined organic layers were washed with water (3 × 30 mL) and brine (30 mL), and dried over $MgSO_4$. The product was isolated by column chromatography using dichloromethane and petroleum ether (v/v = 1:1) to afford 1.744 g orange crystalline solids (94 % yield):

^1H NMR (400 MHz, Chloroform-*d*) δ 9.88 (s, 1H), 7.61 (s, 1H), 7.38 (s, 1H), 7.23 (s, 1H), 7.00 (s, 1H), 2.07 – 1.77 (m, 8H), 1.31 – 0.92 (m, 48H), 0.81 (t, *J* = 7.0 Hz, 12H).

^{13}C NMR (101 MHz, Chloroform-*d*) δ 183.04, 155.42, 155.29, 155.16, 152.73, 152.54, 144.75, 141.58, 138.13, 134.22, 130.67, 125.01, 115.02, 114.09, 113.26, 55.00, 54.23, 39.12, 39.06, 31.93, 30.04, 29.41, 29.33, 24.38, 24.26, 22.74, 14.92.

1,12-bis(5-(2-carbaldehyde-4,4,9,9-tetraoctyl-4,9-dihydro-*s*-indaceno[1,2-*b*:5,6-*b'*]dithiophen-7-yl)thiophen-2-yl)-*para*-carborane (4*p*):

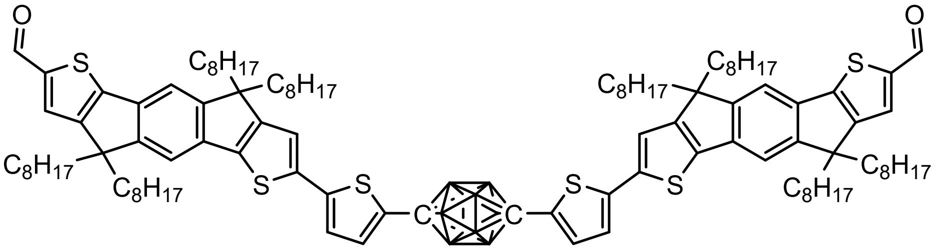

To a mixture of 1,12-di(5-(trimethylstannyl)thiophen-2-yl)-para-carborane (134 mg, 0.211 mmol, 1 eq.), 7-bromo-4,4,9,9-tetraoctyl-4,9-dihydro-*s*-indaceno[1,2-*b*:5,6-*b'*]dithiophene-2-carbaldehyde (was added 434 mg, 0.528 mmol, 2.5 eq.), tris(dibenzylideneacetone)dipalladium(0) (24 mg, 0.0262 mmol, 0.12 eq.), and tris(o-tolyl)phosphine (23.4 mg, 0.0769 mmol, 0.36 eq.) under nitrogen in a microwave pressure tube was added dry toluene (5 mL). The mixture was heated in a microwave reactor with the following programme: 100 °C for 2 minutes, 120 °C for 2 minutes, 140 °C for 2 minutes, 160 °C for 40 minutes. The mixture was then added to 20 mL DCM, washed with water (3 × 15 mL), dried over Na_2SO_4. The solvent was removed under reduced pressure, and the product was purified using recycling preparative GPC in THF, to obtain 194 mg red solids (51 % yield).

^1H NMR (400 MHz, CD_2Cl_2) δ 9.87 (s, 2H), 7.64 (s, 2H), 7.46 (s, 2H), 7.33 (s, 2H), 7.04 (s, 2H), 6.91 (d, *J* = 3.8 Hz, 2H), 6.73 (d, *J* = 3.8 Hz, 2H), 3.55 – 1.53 (m, 10H), 2.10 – 1.85 (m, 16H), 1.24 – 1.03 (m, 96H), 0.83 – 0.78 (m, 24H).

^{13}C NMR (101 MHz, CD_2Cl_2) δ 183.16, 157.49, 155.74, 155.44, 153.83, 152.41, 145.15, 141.10, 139.37, 139.12, 138.48, 138.40, 134.69, 131.08, 127.82, 125.81, 122.99, 119.23, 115.22, 113.70, 54.75, 54.57, 39.37, 32.20, 30.47, 30.27, 29.66, 29.57, 24.59, 24.49, 23.01, 14.24.

^{11}B NMR (128 MHz, CD_2Cl_2) δ -12.00 (d, *J* = 166.6 Hz).

APCI-MS: $C_{108}H_{161}{}^{10}BB_9O_2S_6$ *m/z* 1791.1899 (M+H, theoretical 1791.1852).

1,7-bis(5-(2-carbaldehyde-4,4,9,9-tetraoctyl-4,9-dihydro-*s*-indaceno[1,2-*b*:5,6-*b'*]dithiophen-7-yl)thiophen-2-yl)-*meta*-carborane (4*m*):

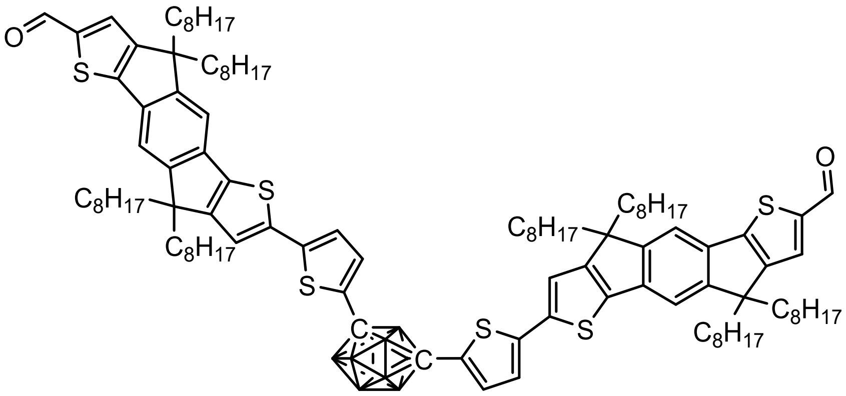

The synthesis was identical to that of 1,12-bis(5-(2-carbaldehyde-4,4,9,9-tetraoctyl-4,9-dihydro-*s*-indaceno[1,2-*b*:5,6-*b'*]dithiophen-7-yl)thiophen-2-yl)-*para*-carborane, using 1,7-di(thiophen-2-yl)-*meta*-carborane instead, to afford the product as red solids (57 % yield):

^{1}H NMR (400 MHz, CD_2Cl_2) δ 9.88 (s, 2H), 7.65 (s, 2H), 7.48 (s, 2H), 7.36 (s, 2H), 7.11 (s, 2H), 7.01 – 6.97 (m, 4H), 3.91 – 1.71 (m, 10H), 2.12 – 1.87 (m, 16H), 1.26 – 1.04 (m, 96H), 0.85 – 0.78 (m, 48H).

^{13}C NMR (101 MHz, CD_2Cl_2) δ 183.11, 157.54, 155.79, 155.50, 153.91, 152.36, 145.28, 141.34, 139.78, 139.02, 138.37, 136.86, 134.83, 131.03, 128.79, 123.15, 119.42, 115.28, 113.79, 73.26, 54.81, 54.62, 54.24, 39.42, 32.24, 30.33, 29.70, 29.63, 29.61, 24.65, 24.56, 23.06, 23.05, 14.30.

^{11}B NMR (128 MHz, CD_2Cl_2) δ 24.71 – -42.31

APCI-MS: $C_{108}H_{161}{}^{10}BB_9O_2S_6$ *m/z* 1791.0836 (M+H, theoretical 1791.1852).

1,2-bis(5-(2-carbaldehyde-4,4,9,9-tetraoctyl-4,9-dihydro-*s*-indaceno[1,2-*b*:5,6-*b'*]dithiophen-7-yl)thiophen-2-yl)-*ortho*-carborane (4*o*):

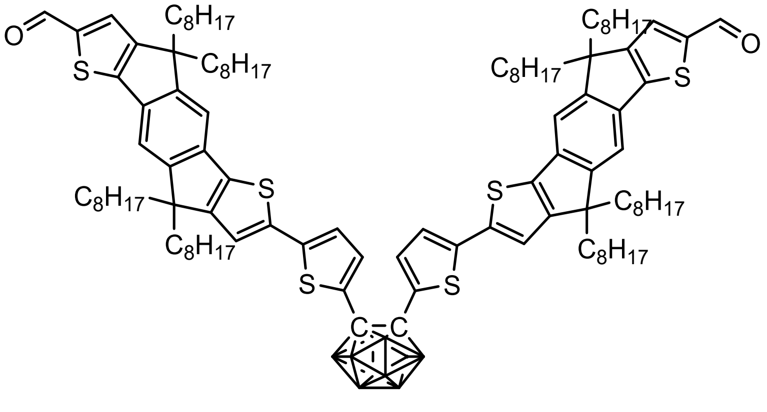

The synthesis was identical to that of 1,12-bis(5-(2-carbaldehyde-4,4,9,9-tetraoctyl-4,9-dihydro-*s*-indaceno[1,2-*b*:5,6-*b'*]dithiophen-7-yl)thiophen-2-yl)-*para*-carborane, using 1,2-di(thiophen-2-yl)-*ortho*-carborane instead, to afford the product as red solids (60 % yield):

^{1}H NMR (400 MHz, CD_2Cl_2) δ 9.86 (s, 2H), 7.63 (s, 2H), 7.45 (s, 2H), 7.32 (s, 2H), 7.19 (d, *J* = 4.0 Hz, 2H), 7.11 (s, 2H), 6.99 (d, *J* = 3.9 Hz, 2H), 3.44-1.58 (m, 10H), 2.09 – 1.79 (m, 16H), 1.23 – 1.01 (m, 96H), 0.82-0.76 (m, 24H).

^{13}C NMR (101 MHz, CD_2Cl_2) δ 183.17, 158.20, 157.50, 155.84, 155.47, 153.93, 152.23, 145.31, 143.11, 142.09, 138.40, 138.08, 135.01, 133.93, 132.59, 131.05, 123.15, 119.96, 115.28, 113.87, 82.48, 68.17, 54.79, 54.58, 39.33, 32.18, 30.27, 30.23, 29.65, 29.60, 29.56, 25.99, 24.60, 24.47, 23.01, 14.26.

^{11}B NMR (128 MHz, CD_2Cl_2) δ 23.31 – -39.10 (m).

APCI-MS: $C_{108}H_{161}{}^{10}BB_9O_2S_6$ *m/z* 1791.1810 (M+H, theoretical 1791.1852).

1,12-bis(5-((*Z*)-2-((1-(dicyanomethylene)-3-oxo-1,3-dihydro-2*H*-inden-2-ylidene)methyl)-4,4,9,9-tetraoctyl-4,9-dihydro-*s*-indaceno[1,2-*b*:5,6-*b′*]dithiophen-7-yl)thiophen-2-yl)-*para*-carborane (*p*Cb(T-IDIC)$_2$):

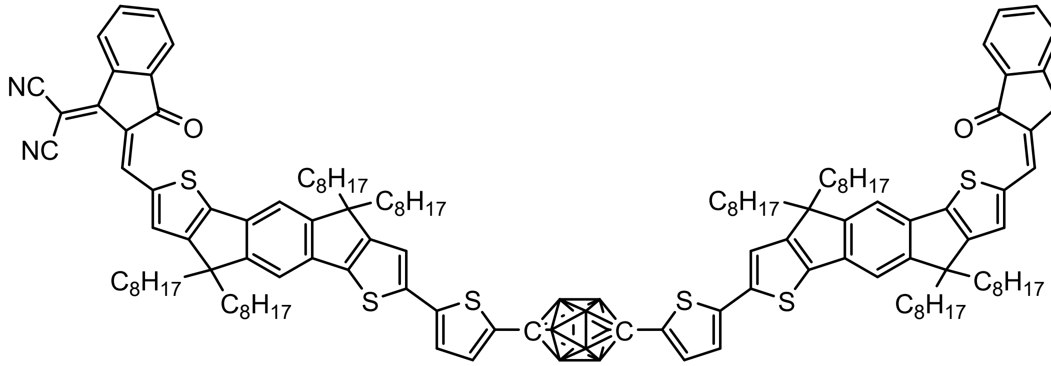

To a mixture of 1,12-bis(5-(2-carbaldehyde-4,4,9,9-tetraoctyl-4,9-dihydro-*s*-indaceno[1,2-*b*:5,6-*b′*]dithiophen-7-yl)thiophen-2-yl)-*para*-carborane (94 mg, 0.0525 mmol, 1 eq.) and 2-(3-oxo-2,3-dihydroinden-1-ylidene)malononitrile (56 mg, 0.288 mmol, 5.5 eq.) under nitrogen was added dry chloroform (20 mL), followed by dropwise addition of pyridine (0.07 mL). The mixture wasrefluxed for 12 hours. After cooling to room temperature, the crude mixture was filtered over a plug of silica, eluting with DCM. The solvent was removed under reduced pressure, and the product was purified using recycling preparative GPC in THF, to obtain 106 mg metallic red solids (94%).

^{1}H NMR (400 MHz, CD_2Cl_2) δ 8.97 (s, 2H), 8.67 (d, *J* = 7.4 Hz, 2H), 7.90 (d, *J* = 6.8 Hz, 2H), 7.80 – 7.68 (m, 6H), 7.62 (s, 2H), 7.36 (s, 2H), 7.07 (s, 2H), 6.94 (d, *J* = 3.9 Hz, 2H), 6.74 (d, *J* = 3.9 Hz, 2H), 3.44 – 1.83 (m, 10H), 2.15 – 1.88 (m, 16H), 1.26 – 1.05 (m, 96H), 0.84 – 0.77 (m, 24H).

^{13}C NMR (101 MHz, CD_2Cl_2) δ 188.62, 162.98, 161.17, 158.60, 157.02, 156.83, 154.34, 141.02, 140.41, 140.26, 140.22, 139.21, 138.78, 138.58, 137.38, 135.14, 134.83, 134.53, 127.88, 125.43, 123.73, 123.28, 121.16, 119.24, 116.27, 115.55, 113.83, 68.23, 54.77, 54.60, 39.56, 39.34, 32.22, 32.19, 30.29, 29.67, 29.60, 24.68, 24.56, 23.04, 23.01, 14.26.

^{11}B NMR (128 MHz, CD_2Cl_2) δ -11.98 (d, *J* = 166.9 Hz).

MALDI: $C_{132}B_{10}H_{168}N_4O_2S_6$ *m/z* 2142.3 (M+, exact mass 2143.24).

1,7-bis(5-((*Z*)-2-((1-(dicyanomethylene)-3-oxo-1,3-dihydro-2*H*-inden-2-ylidene)methyl)-4,4,9,9-tetraoctyl-4,9-dihydro-*s*-indaceno[1,2-*b*:5,6-*b′*]dithiophen-7-yl)thiophen-2-yl)-*meta*-carborane (*m*Cb(T-IDIC)$_2$):

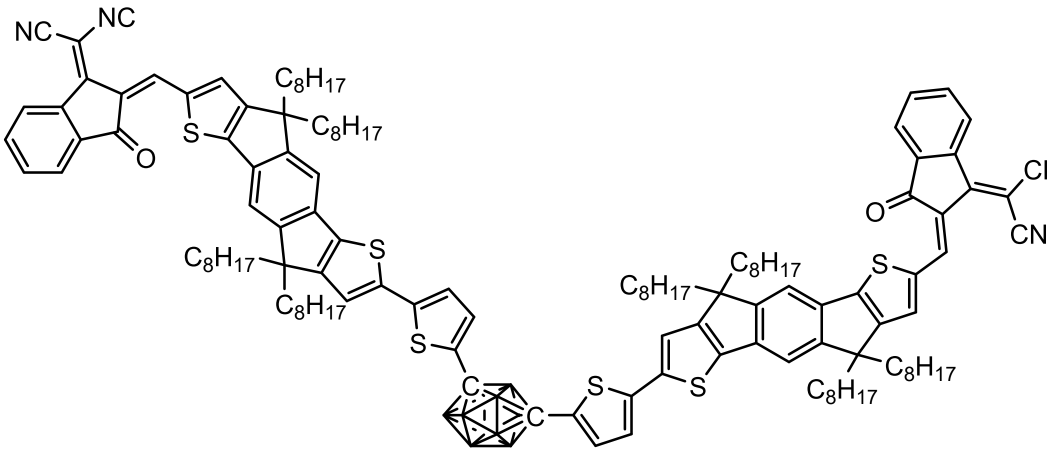

The synthesis was identical to that of 1,12-bis(5-((*Z*)-2-((1-(dicyanomethylene)-3-oxo-1,3-dihydro-2*H*-inden-2-ylidene)methyl)-4,4,9,9-tetraoctyl-4,9-dihydro-*s*-indaceno[1,2-*b*:5,6-*b'*]dithiophen-7-yl)thiophen-2-yl)-*para*-carborane, using 1,7-bis(5-(2-carbaldehyde-4,4,9,9-tetraoctyl-4,9-dihydro-*s*-indaceno[1,2-*b*:5,6-*b'*]dithiophen-7-yl)thiophen-2-yl)-*meta*-carborane instead, to afford the product as metallic red solids (82 % yield):

^{1}H NMR (400 MHz, CD_2Cl_2) δ 8.97 (s, 2H), 8.67 (d, *J* = 7.4 Hz, 2H), 7.89 (d, *J* = 7.0 Hz, 2H), 7.79 – 7.70 (m, 6H), 7.65 (s, 2H), 7.39 (s, 2H), 7.14 (s, 2H), 7.06 – 6.96 (m, 4H), 3.99 – 1.82 (m, 10H), 2.16 – 1.91 (m, 16H), 1.26 – 1.06 (m, 96H), 0.81 (t, *J* = 6.9 Hz, 24H).

^{13}C NMR (101 MHz, CD_2Cl_2) δ ^{13}C NMR (101 MHz, CD_2Cl_2) δ 188.65, 162.89, 161.21, 158.59, 157.01, 156.84, 154.35, 141.22, 140.41, 140.18, 140.01, 139.59, 138.78, 138.57, 137.39, 137.12, 135.15, 134.90, 134.55, 128.84, 125.44, 123.73, 123.41, 121.21, 119.42, 116.28, 115.53, 113.87, 73.19, 68.26, 54.80, 54.61, 39.55, 39.33, 32.20, 30.28, 29.66, 29.59, 24.67, 24.56, 23.03, 23.00, 14.24.

^{11}B NMR (128 MHz, CD_2Cl_2) δ 21.43 – -38.61 (m).

MALDI: $C_{132}B_{10}H_{168}N_4O_2S_6$ *m/z* 2143.1 (M+, exact mass 2143.24).

1,2-bis(5-((*Z*)-2-((1-(dicyanomethylene)-3-oxo-1,3-dihydro-2*H*-inden-2-ylidene)methyl)-4,4,9,9-tetraoctyl-4,9-dihydro-*s*-indaceno[1,2-*b*:5,6-*b'*]dithiophen-7-yl)thiophen-2-yl)-*ortho*-carborane (*o*Cb(T-IDIC)$_2$):

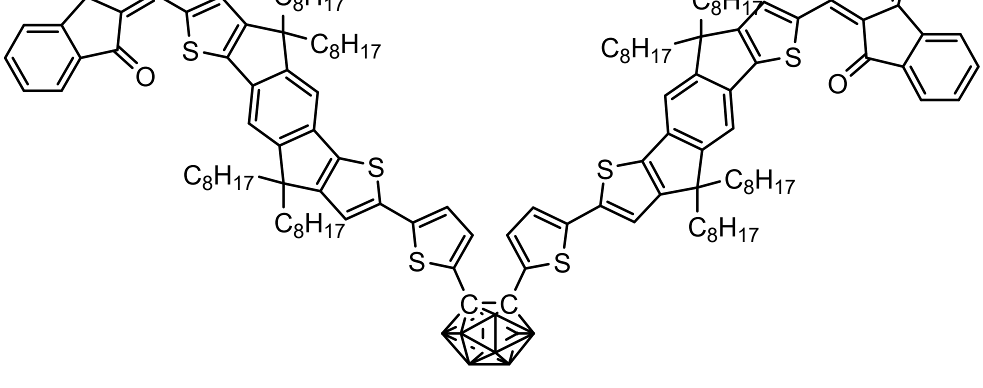

The synthesis was identical to that of 1,12-bis(5-((*Z*)-2-((1-(dicyanomethylene)-3-oxo-1,3-dihydro-2*H*-inden-2-ylidene)methyl)-4,4,9,9-tetraoctyl-4,9-dihydro-*s*-indaceno[1,2-*b*:5,6-*b'*]dithiophen-7-yl)thiophen-2-yl)-*para*-carborane, using 1,2-bis(5-(2-carbaldehyde-4,4,9,9-tetraoctyl-4,9-dihydro-*s*-indaceno[1,2-*b*:5,6-*b'*]dithiophen-7-yl)thiophen-2-yl)-*ortho*-carborane instead, to afford the product as metallic red solids (65 % yield):

^{1}H NMR (400 MHz, CD_2Cl_2) δ 8.96 (s, 2H), 8.67 (d, *J* = 7.5 Hz, 2H), 7.89 (d, *J* = 6.9 Hz, 2H), 7.79 – 7.68 (m, 6H), 7.63 (s, 2H), 7.36 (s, 2H), 7.22 (d, *J* = 4.0 Hz, 2H), 7.15 (s, 2H), 7.02 (d, *J* = 3.9 Hz, 2H), 3.63 – 1.70 (m, 10H), 2.12 – 1.82 (m, 16H), 1.26 – 1.02 (m, 96H), 0.83 – 0.76 (m, 24H).

^{13}C NMR (101 MHz, CD_2Cl_2) δ 188.57, 162.65, 161.06, 158.54, 156.99, 156.86, 154.42, 142.93, 141.98, 140.53, 140.37, 139.86, 139.42, 138.75, 138.56, 137.36, 135.15, 134.55, 133.96, 132.88, 125.44, 123.75, 123.41, 121.30, 119.96, 116.32, 115.50, 115.47, 114.01, 82.38, 68.41, 54.81, 54.61, 39.52, 39.30, 32.19, 30.27, 29.66, 29.62, 29.59, 24.68, 24.54, 23.03, 23.01, 14.30, 14.27, 1.19.

^{11}B NMR (128 MHz, CD_2Cl_2) δ 23.22 – -34.91 (m).

MALDI: $C_{132}B_{10}H_{168}N_4O_2S_6$ *m/z* 2143.7 (M+, exact mass 2143.24).

1,2-bis(5-((*Z*)-2-((1-(dicyanomethylene)-5,6-difluoro-3-oxo-1,3-dihydro-2*H*-inden-2-ylidene)methyl)-4,4,9,9-tetraoctyl-4,9-dihydro-*s*-indaceno[1,2-*b*:5,6-*b'*]dithiophen-7-yl)thiophen-2-yl)-*ortho*-carborane (*o*Cb(T-IDIC)$_2$-4F):

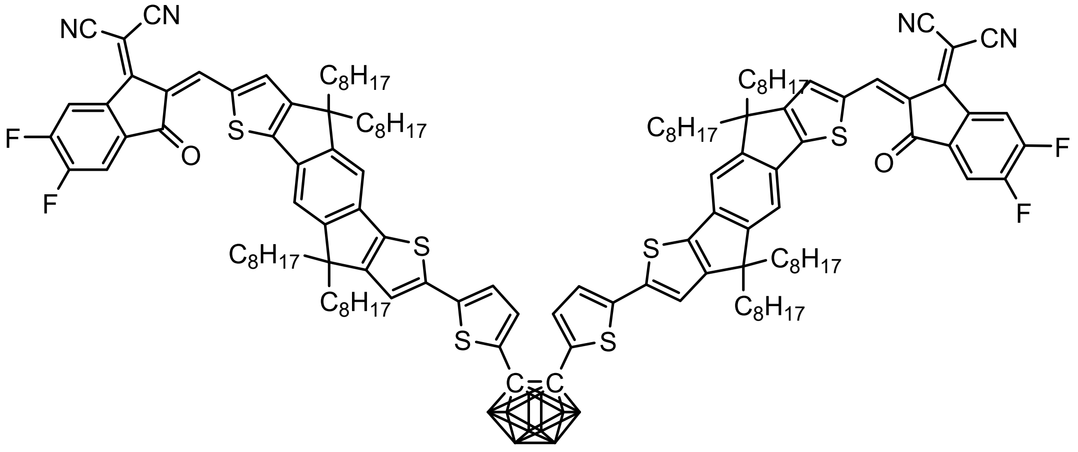

The synthesis was identical to that of 1,12-bis(5-((*Z*)-2-((1-(dicyanomethylene)-3-oxo-1,3-dihydro-2*H*-inden-2-ylidene)methyl)-4,4,9,9-tetraoctyl-4,9-dihydro-*s*-indaceno[1,2-*b*:5,6-*b'*]dithiophen-7-yl)thiophen-2-yl)-*para*-carborane, using 1,2-bis(5-(2-carbaldehyde-4,4,9,9-tetraoctyl-4,9-dihydro-*s*-indaceno[1,2-*b*:5,6-*b'*]dithiophen-7-yl)thiophen-2-yl)-*ortho*-carborane and 2-(5,6-difluoro-3-oxo-2,3-dihydroinden-1-ylidene)malononitrile instead, to afford the product as metallic red solids (90 % yield):

^{1}H NMR (400 MHz, CD_2Cl_2) δ 8.94 (s, 2H), 8.52 (dd, *J* = 10.2, 6.4 Hz, 2H), 7.76 (s, 2H), 7.68 (t, *J* = 7.6 Hz, 2H), 7.62 (s, 2H), 7.36 (s, 2H), 7.22 (d, *J* = 4.0 Hz, 2H), 7.14 (s, 2H), 7.03 (d, *J* = 4.0 Hz, 2H), 3.70 – 1.75 (m, 10H), 2.14 – 1.87 (m, 16H), 1.25 – 0.99 (m, 96H), 0.82 – 0.74 (m, 24H).

^{13}C NMR (101 MHz, CD_2Cl_2) δ 186.26, 163.97, 158.98, 158.78, 157.30, 157.16, 156.01, 155.91, 155.87, 155.78, 154.52, 153.41, 153.36, 153.27, 153.22, 142.87, 141.90, 140.40, 140.31, 139.69, 139.14, 138.90, 137.04, 137.01, 136.95, 135.06, 135.02, 134.93, 133.97, 132.97, 123.49, 120.29, 119.96, 116.51, 115.26, 115.16, 115.05, 114.03, 112.79, 112.60, 82.33, 68.82, 54.84, 54.64, 39.50, 39.28, 32.18, 30.25, 29.64, 29.61, 29.57, 24.67, 24.53, 23.03, 23.00, 14.28, 14.26.

^{19}F NMR (377 MHz, CD_2Cl_2) δ -122.89 – -123.20 (m), -123.89 – -124.19 (m).

^{11}B NMR (128 MHz, CD_2Cl_2) δ 22.18 – -32.67 (m).

Characterisation

4,4,9,9-tetraoctyl-4,9-dihydro-*s*-indaceno[1,2-*b*:5,6-*b'*]dithiophene-2-carbaldehyde:

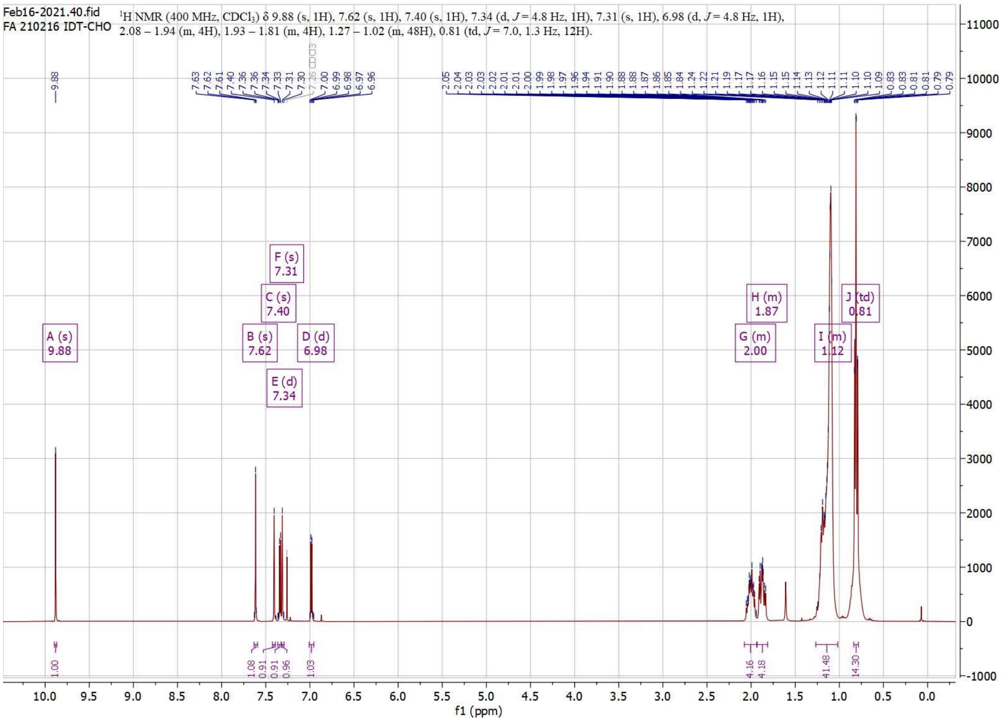

^{1}H NMR (400 MHz, $CDCl_3$) δ 9.88 (s, 1H), 7.62 (s, 1H), 7.40 (s, 1H), 7.34 (d, J = 4.8 Hz, 1H), 7.31 (s, 1H), 6.98 (d, J = 4.8 Hz, 1H), 2.08 – 1.94 (m, 4H), 1.93 – 1.81 (m, 4H), 1.27 – 1.02 (m, 48H), 0.81 (td, J = 7.0, 1.3 Hz, 12H).

Figure S10. ^{1}H NMR spectrum of 4,4,9,9-tetraoctyl-4,9-dihydro-*s*-indaceno[1,2-*b*:5,6-*b'*]dithiophene-2-carbaldehyde

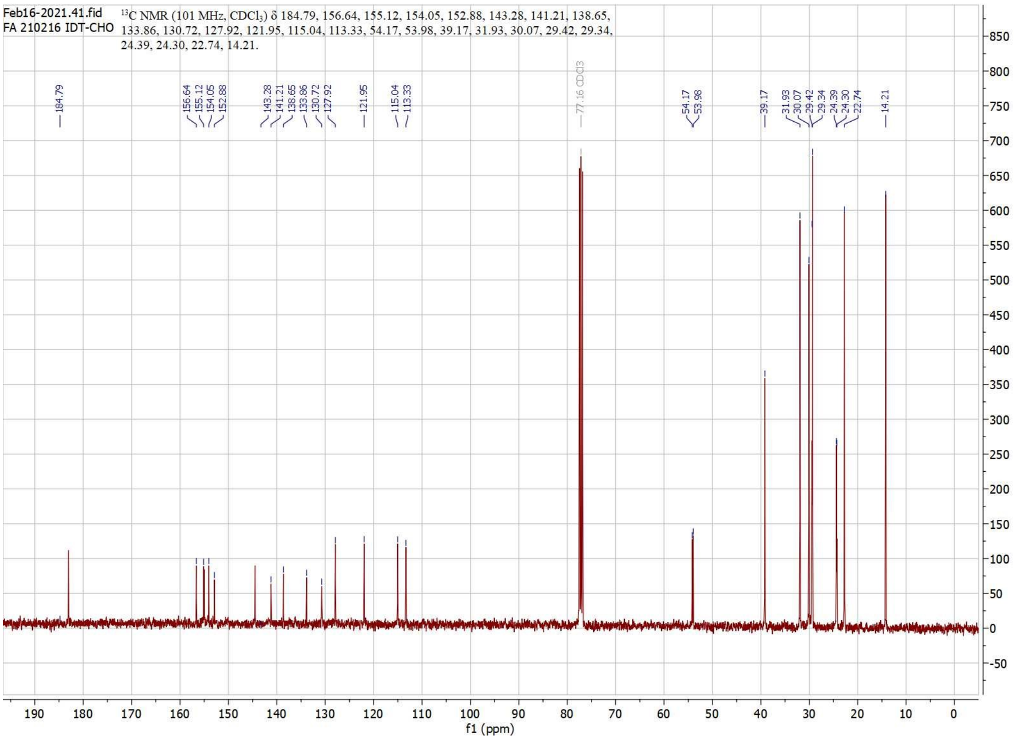

^{13}C NMR (101 MHz, $CDCl_3$) δ 184.79, 156.64, 155.12, 154.05, 152.88, 143.28, 141.21, 138.65, 133.86, 130.72, 127.92, 121.95, 115.04, 113.33, 54.17, 53.98, 39.17, 31.93, 30.07, 29.42, 29.34, 24.39, 24.30, 22.74, 14.21.

Figure S11. ^{11}B NMR spectrum of 4,4,9,9-tetraoctyl-4,9-dihydro-*s*-indaceno[1,2-*b*:5,6-*b'*]dithiophene-2-carbaldehyde

7-bromo-4,4,9,9-tetraoctyl-4,9-dihydro-*s*-indaceno[1,2-*b*:5,6-*b'*]dithiophene-2-carbaldehyde:

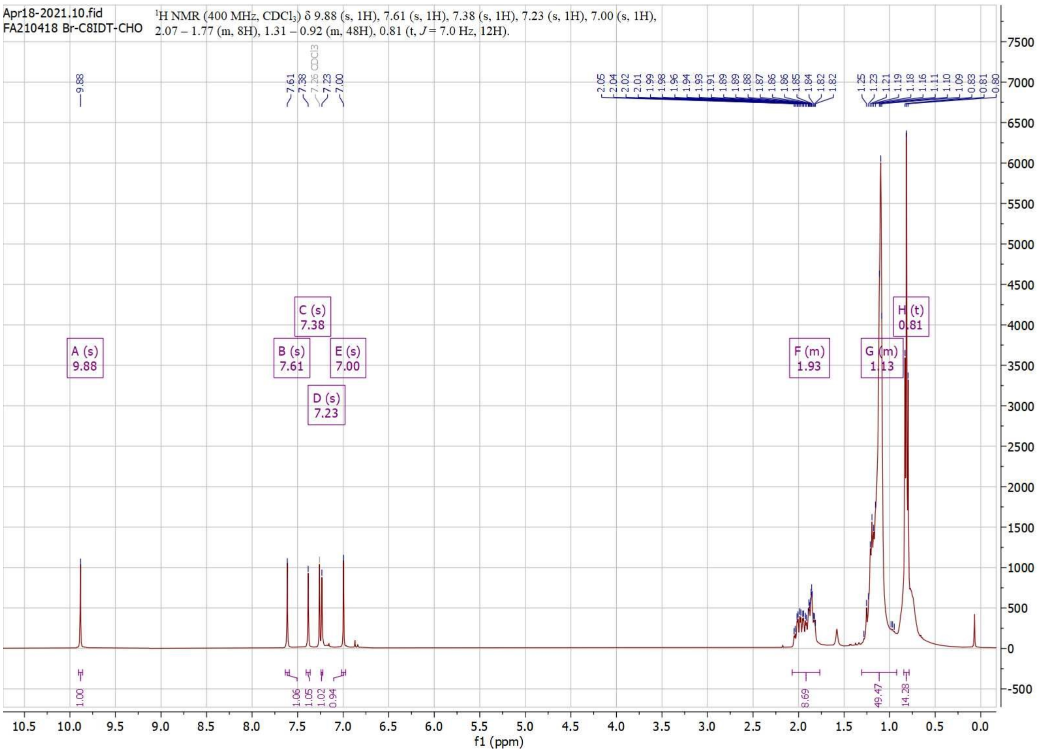

Apr18-2021.10.fid
FA210418 Br-C8IDT-CHO

^{1}H NMR (400 MHz, CDCl$_3$) δ 9.88 (s, 1H), 7.61 (s, 1H), 7.38 (s, 1H), 7.23 (s, 1H), 7.00 (s, 1H), 2.07 – 1.77 (m, 8H), 1.31 – 0.92 (m, 48H), 0.81 (t, J = 7.0 Hz, 12H).

Figure S12. ^{1}H NMR spectrum of *m*CbT2-NDI 7-bromo-4,4,9,9-tetraoctyl-4,9-dihydro-*s*-indaceno[1,2-*b*:5,6-*b'*]dithiophene-2-carbaldehyde.

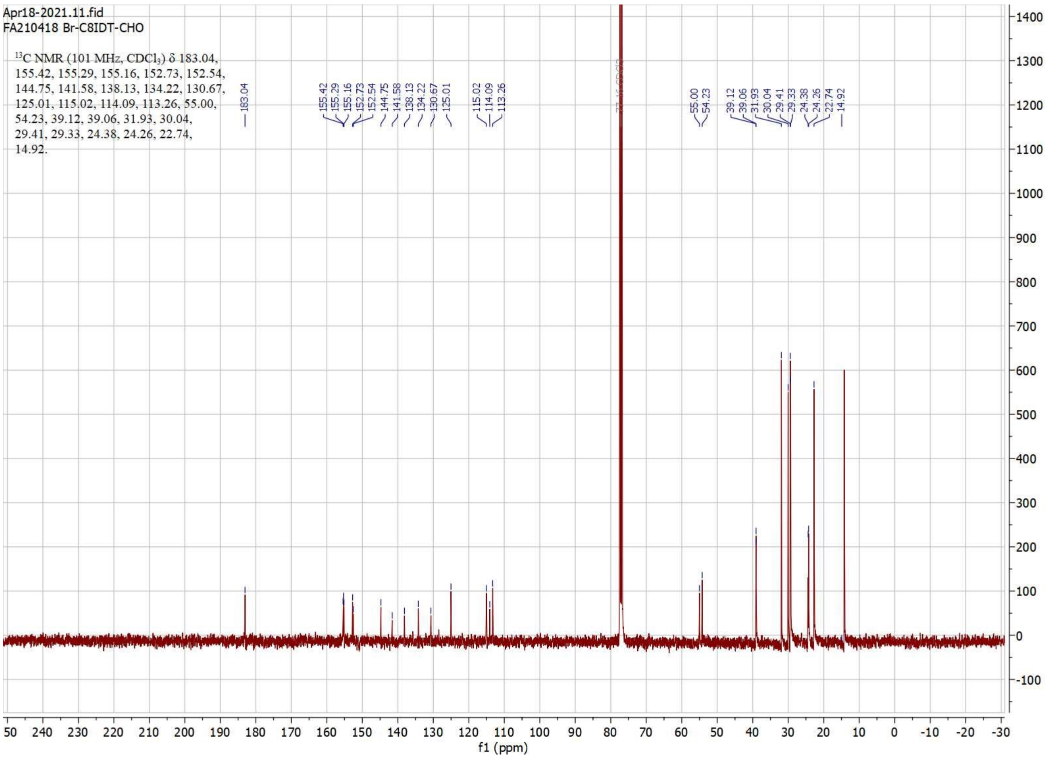

Apr18-2021.11.fid
FA210418 Br-C8IDT-CHO

^{13}C NMR (101 MHz, CDCl$_3$) δ 183.04, 155.42, 155.29, 155.16, 152.73, 152.54, 144.75, 141.58, 138.13, 134.22, 130.67, 125.01, 115.02, 114.09, 113.26, 55.00, 54.23, 39.12, 39.06, 31.93, 30.04, 29.41, 29.33, 24.38, 24.26, 22.74, 14.92.

Figure S13. ^{13}C NMR spectrum of 7-bromo-4,4,9,9-tetraoctyl-4,9-dihydro-*s*-indaceno[1,2-*b*:5,6-*b'*]dithiophene-2-carbaldehyde.

1,12-bis(5-(2-carbaldehyde-4,4,9,9-tetraoctyl-4,9-dihydro-*s*-indaceno[1,2-*b*:5,6-*b'*]dithiophen-7-yl)thiophen-2-yl)-*para*-carborane:

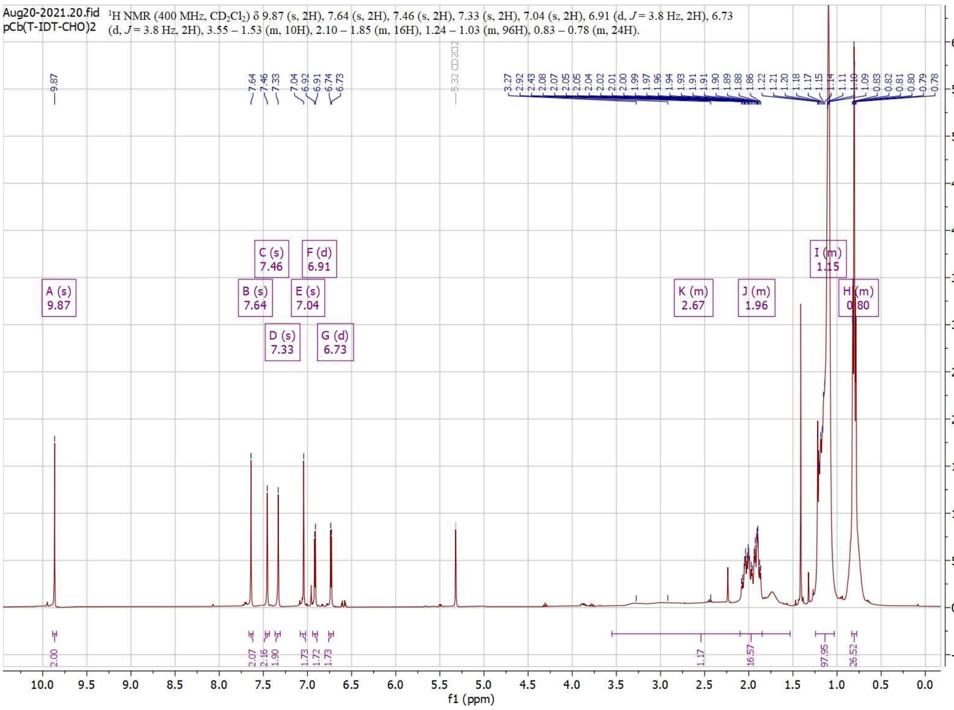

^{1}H NMR (400 MHz, CD_2Cl_2) δ 9.87 (s, 2H), 7.64 (s, 2H), 7.46 (s, 2H), 7.33 (s, 2H), 7.04 (s, 2H), 6.91 (d, J = 3.8 Hz, 2H), 6.73 (d, J = 3.8 Hz, 2H), 3.55 – 1.53 (m, 10H), 2.10 – 1.85 (m, 16H), 1.24 – 1.03 (m, 96H), 0.83 – 0.78 (m, 24H).

Figure S14. ^{1}H NMR spectrum of 1,12-bis(5-(2-carbaldehyde-4,4,9,9-tetraoctyl-4,9-dihydro-*s*-indaceno[1,2-*b*:5,6-*b'*]dithiophen-7-yl)thiophen-2-yl)-*para*-carborane.

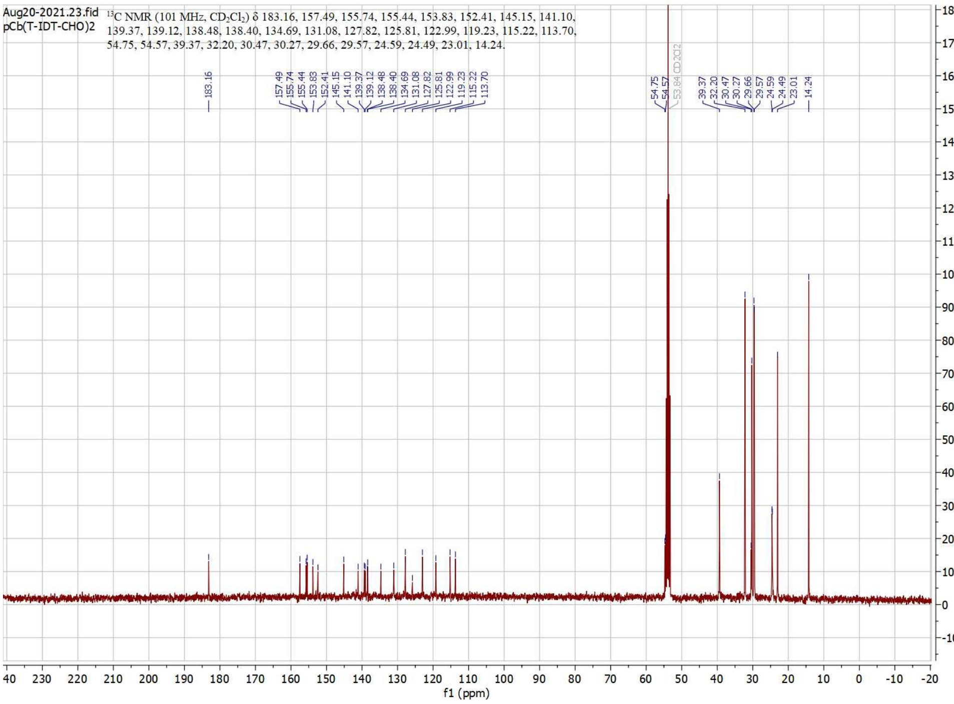

^{13}C NMR (101 MHz, CD_2Cl_2) δ 183.16, 157.49, 155.74, 155.44, 153.83, 152.41, 145.15, 141.10, 139.37, 139.12, 138.48, 138.40, 134.69, 131.08, 127.82, 125.81, 122.99, 119.23, 115.22, 113.70, 54.75, 54.57, 39.37, 32.20, 30.47, 30.27, 29.66, 29.57, 24.59, 24.49, 23.01, 14.24.

Figure S15. ^{13}C NMR spectrum of 1,12-bis(5-(2-carbaldehyde-4,4,9,9-tetraoctyl-4,9-dihydro-*s*-indaceno[1,2-*b*:5,6-*b'*]dithiophen-7-yl)thiophen-2-yl)-*para*-carborane.

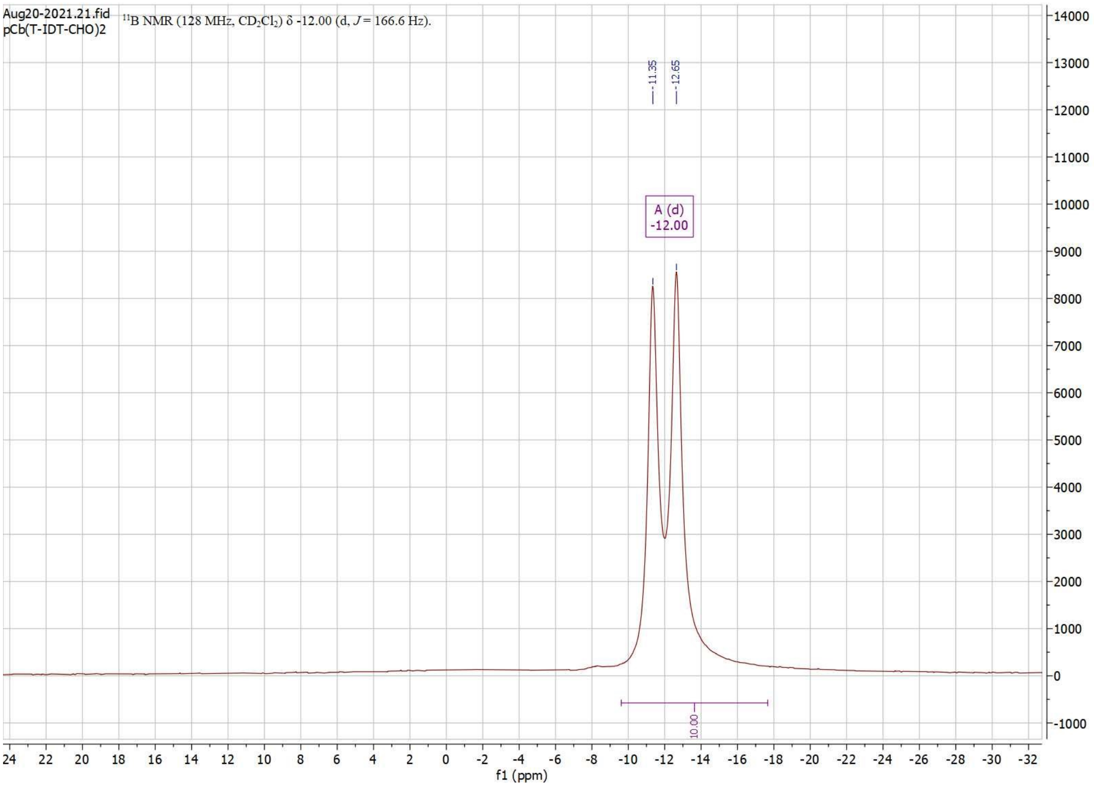

Figure S16. ^{11}B NMR spectrum of 1,12-bis(5-(2-carbaldehyde-4,4,9,9-tetraoctyl-4,9-dihydro-*s*-indaceno[1,2-*b*:5,6-*b′*]dithiophen-7-yl)thiophen-2-yl)-*para*-carborane.

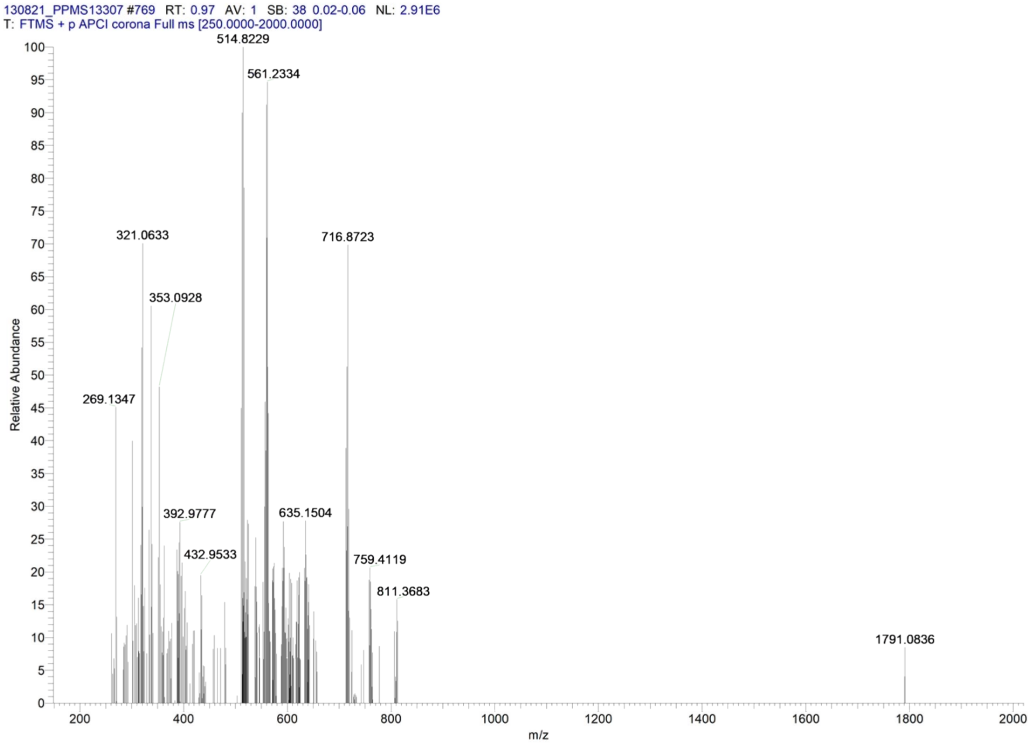

Figure S17. APCI-MS of 1,12-bis(5-(2-carbaldehyde-4,4,9,9-tetraoctyl-4,9-dihydro-*s*-indaceno[1,2-*b*:5,6-*b′*]dithiophen-7-yl)thiophen-2-yl)-*para*-carborane.

1,7-bis(5-(2-carbaldehyde-4,4,9,9-tetraoctyl-4,9-dihydro-*s*-indaceno[1,2-*b*:5,6-*b′*]dithiophen-7-yl)thiophen-2-yl)-*meta*-carborane:

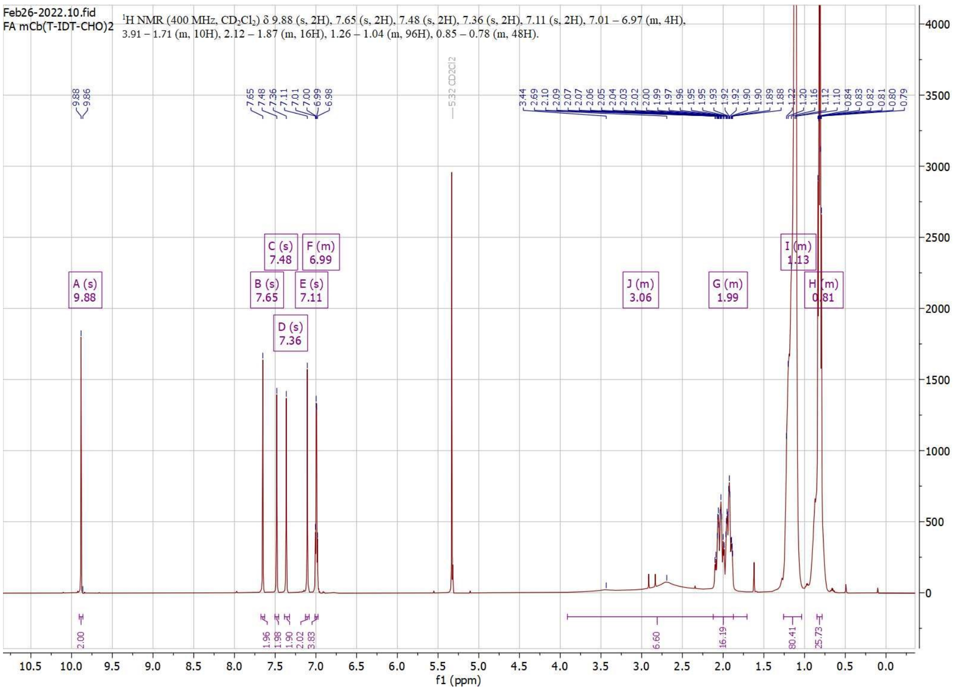

^{1}H NMR (400 MHz, CD_2Cl_2) δ 9.88 (s, 2H), 7.65 (s, 2H), 7.48 (s, 2H), 7.36 (s, 2H), 7.11 (s, 2H), 7.01 – 6.97 (m, 4H), 3.91 – 1.71 (m, 10H), 2.12 – 1.87 (m, 16H), 1.26 – 1.04 (m, 96H), 0.85 – 0.78 (m, 48H).

Figure S18. ^{1}H NMR spectrum of 1,7-bis(5-(2-carbaldehyde-4,4,9,9-tetraoctyl-4,9-dihydro-*s*-indaceno[1,2-*b*:5,6-*b′*]dithiophen-7-yl)thiophen-2-yl)-*meta*-carborane.

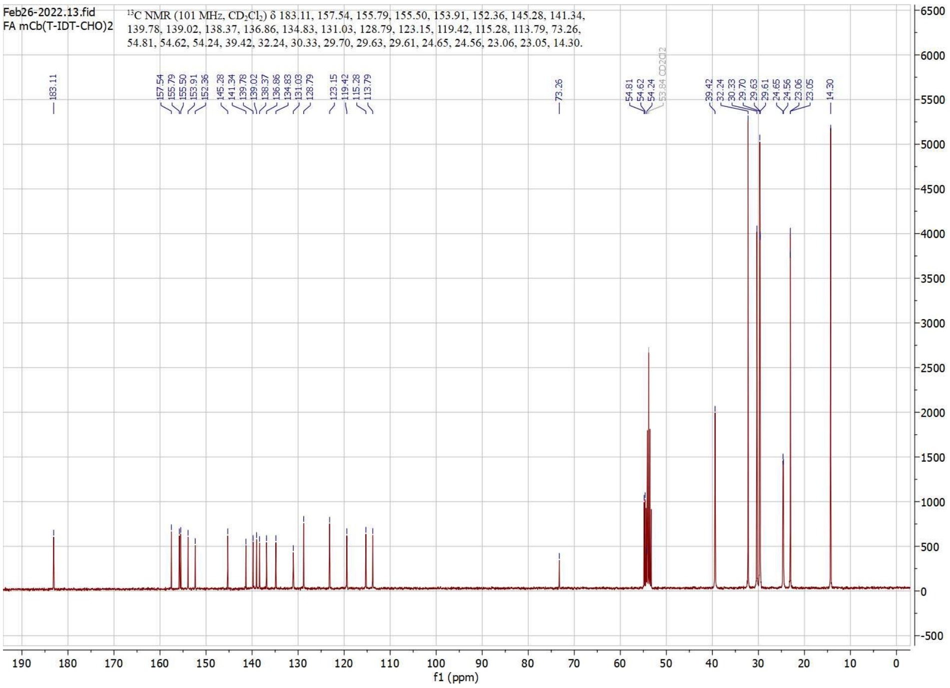

^{13}C NMR (101 MHz, CD_2Cl_2) δ 183.11, 157.54, 155.79, 155.50, 153.91, 152.36, 145.28, 141.34, 139.78, 139.02, 138.37, 136.86, 134.83, 131.03, 128.79, 123.15, 119.42, 115.28, 113.79, 73.26, 54.81, 54.62, 54.24, 39.42, 32.24, 30.33, 29.70, 29.63, 29.61, 24.65, 24.56, 23.06, 23.05, 14.30.

Figure S19. ^{13}C NMR spectrum of 1,7-bis(5-(2-carbaldehyde-4,4,9,9-tetraoctyl-4,9-dihydro-*s*-indaceno[1,2-*b*:5,6-*b′*]dithiophen-7-yl)thiophen-2-yl)-*meta*-carborane.

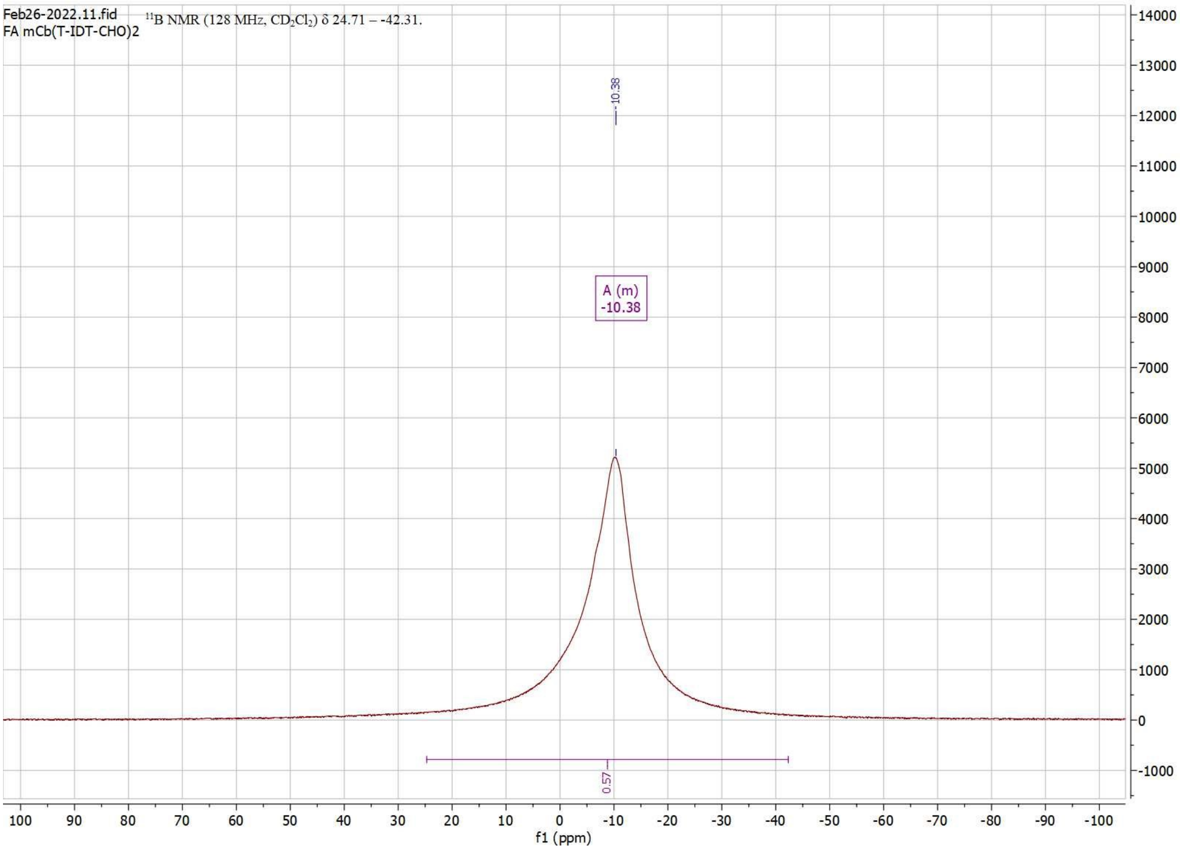

Figure S20. ^{11}B NMR spectrum of 1,7-bis(5-(2-carbaldehyde-4,4,9,9-tetraoctyl-4,9-dihydro-*s*-indaceno[1,2-*b*:5,6-*b'*]dithiophen-7-yl)thiophen-2-yl)-*meta*-carborane.

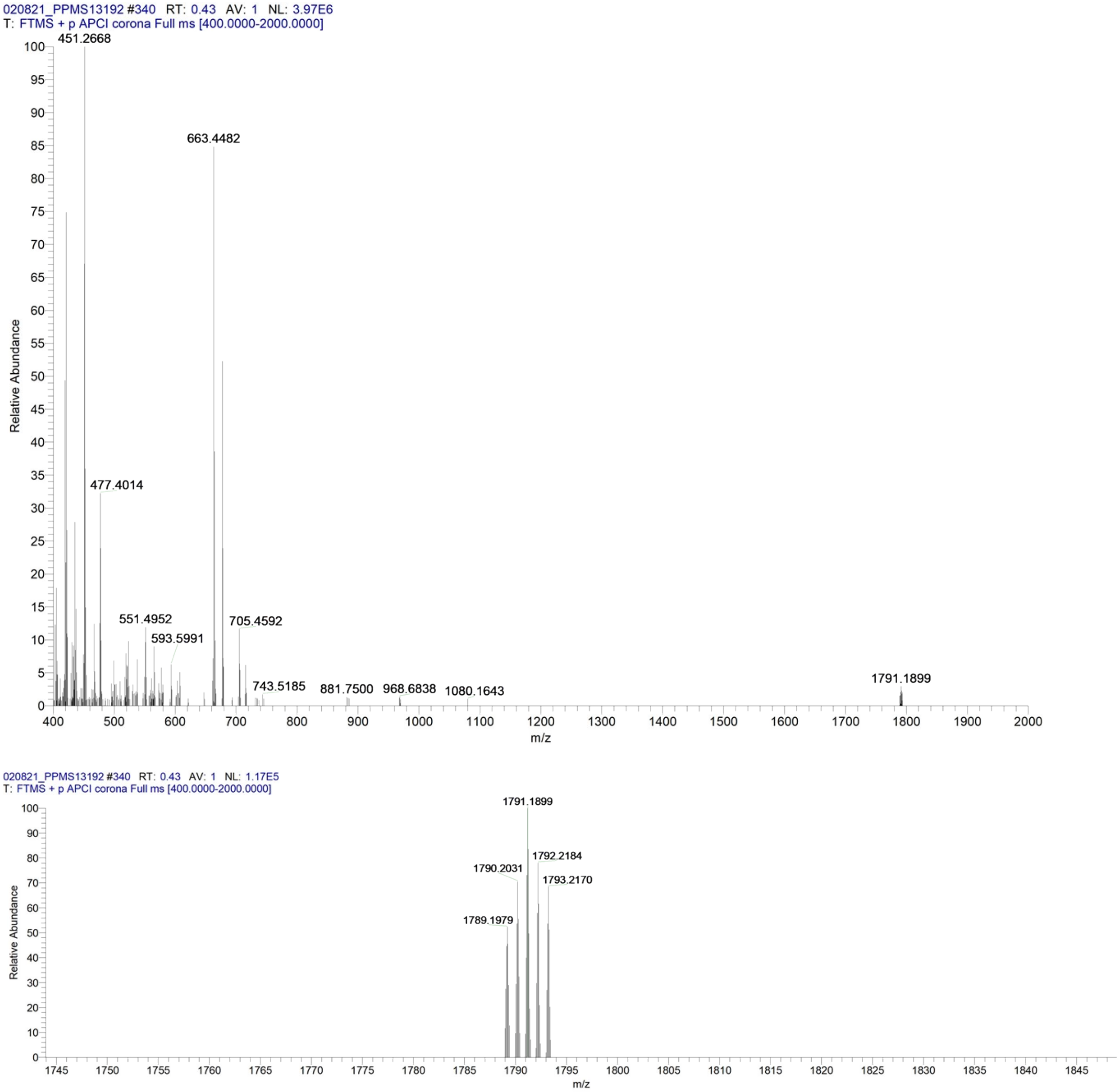

Figure S21. APCI-MS of 1,7-bis(5-(2-carbaldehyde-4,4,9,9-tetraoctyl-4,9-dihydro-*s*-indaceno[1,2-*b*:5,6-*b'*]dithiophen-7-yl)thiophen-2-yl)-*meta*-carborane.

1,2-bis(5-(2-carbaldehyde-4,4,9,9-tetraoctyl-4,9-dihydro-*s*-indaceno[1,2-*b*:5,6-*b′*]dithiophen-7-yl)thiophen-2-yl)-*ortho*-carborane:

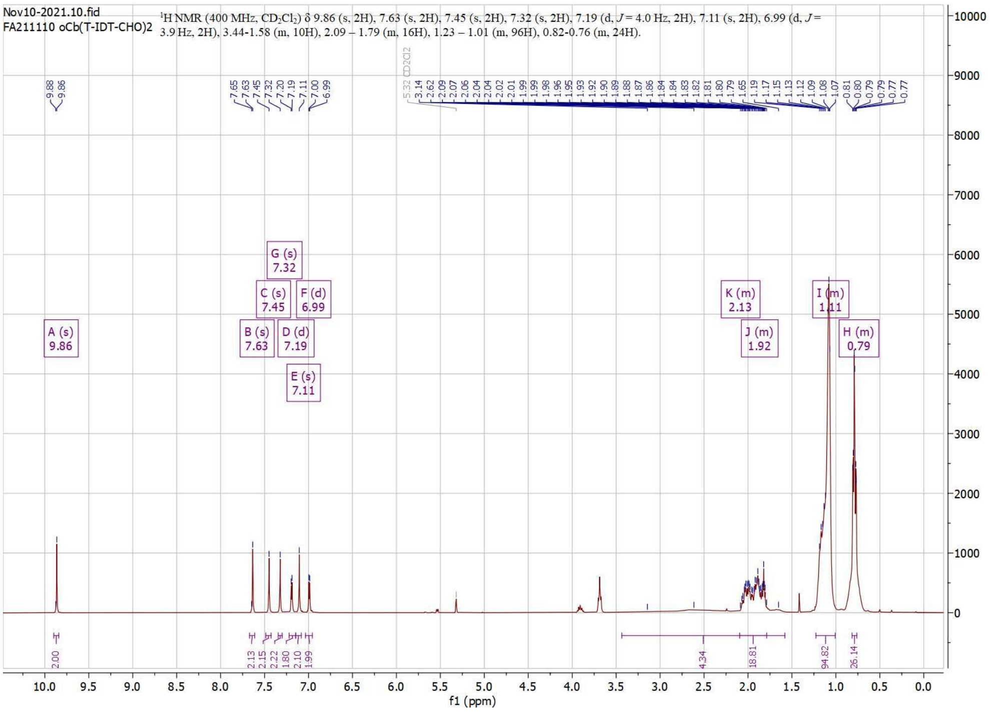

^{1}H NMR (400 MHz, CD_2Cl_2) δ 9.86 (s, 2H), 7.63 (s, 2H), 7.45 (s, 2H), 7.32 (s, 2H), 7.19 (d, J = 4.0 Hz, 2H), 7.11 (s, 2H), 6.99 (d, J = 3.9 Hz, 2H), 3.44-1.58 (m, 10H), 2.09 – 1.79 (m, 16H), 1.23 – 1.01 (m, 96H), 0.82-0.76 (m, 24H).

Figure S22. ^{1}H NMR spectrum of 1,2-bis(5-(2-carbaldehyde-4,4,9,9-tetraoctyl-4,9-dihydro-*s*-indaceno[1,2-*b*:5,6-*b′*]dithiophen-7-yl)thiophen-2-yl)-*ortho*-carborane.

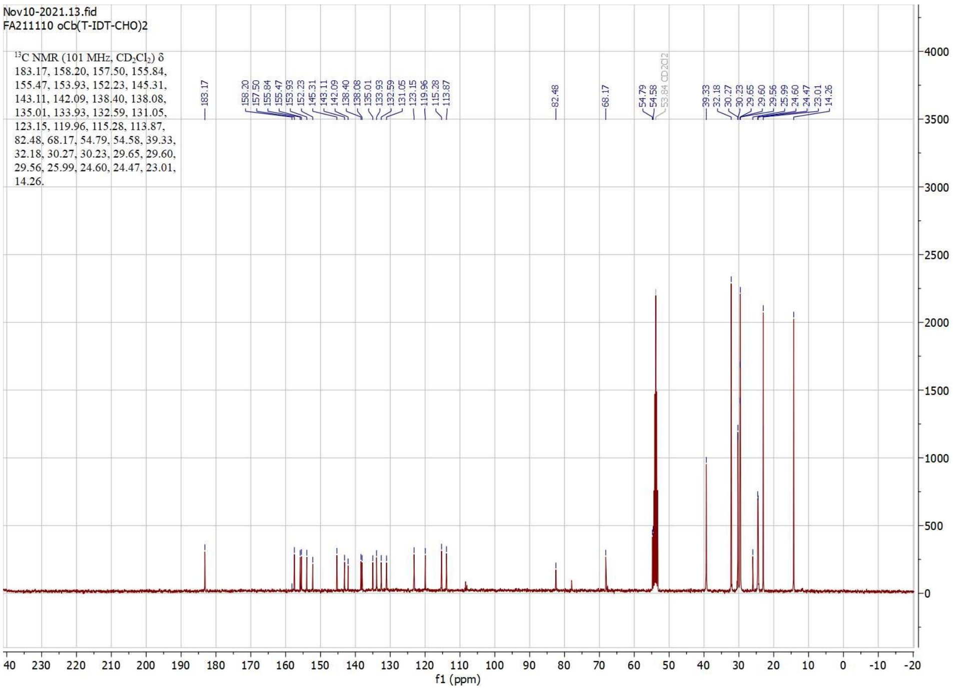

^{13}C NMR (101 MHz, CD_2Cl_2) δ 183.17, 158.20, 157.50, 155.84, 155.47, 153.93, 152.23, 145.31, 143.11, 142.09, 138.40, 138.08, 135.01, 133.93, 132.59, 131.05, 123.15, 119.96, 115.28, 113.87, 82.48, 68.17, 54.79, 54.58, 39.33, 32.18, 30.27, 30.23, 29.65, 29.60, 29.56, 25.99, 24.60, 24.47, 23.01, 14.26.

Figure S23. ^{13}C NMR spectrum of 1,2-bis(5-(2-carbaldehyde-4,4,9,9-tetraoctyl-4,9-dihydro-*s*-indaceno[1,2-*b*:5,6-*b′*]dithiophen-7-yl)thiophen-2-yl)-*ortho*-carborane.

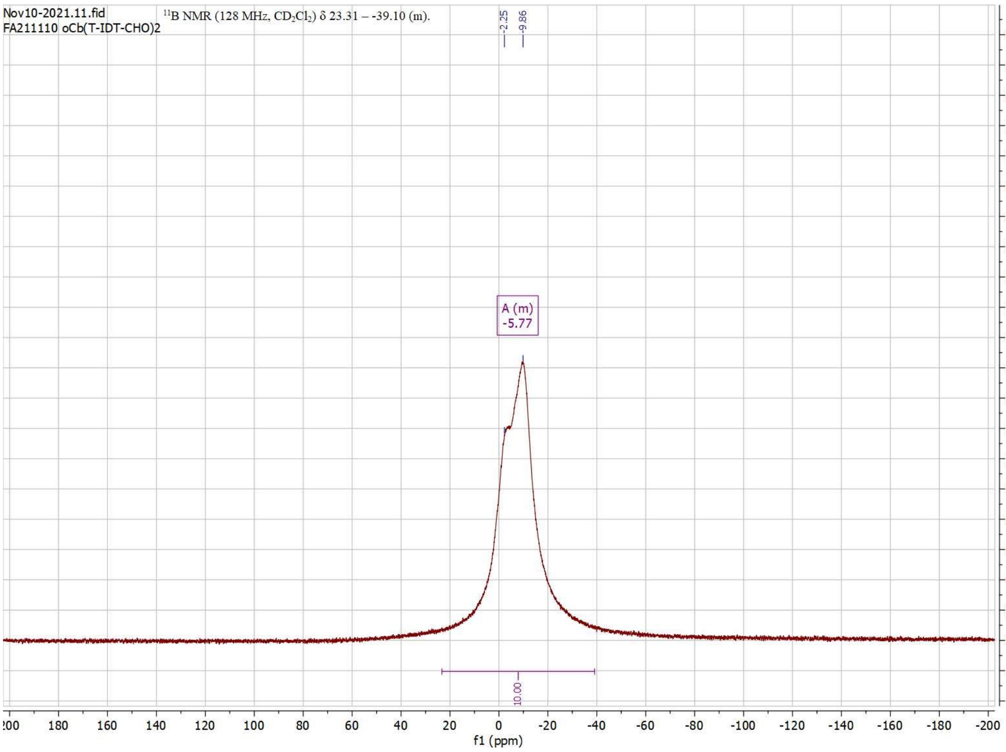

Figure S24. ^{11}B NMR spectrum of 1,2-bis(5-(2-carbaldehyde-4,4,9,9-tetraoctyl-4,9-dihydro-*s*-indaceno[1,2-*b*:5,6-*b′*]dithiophen-7-yl)thiophen-2-yl)-*ortho*-carborane.

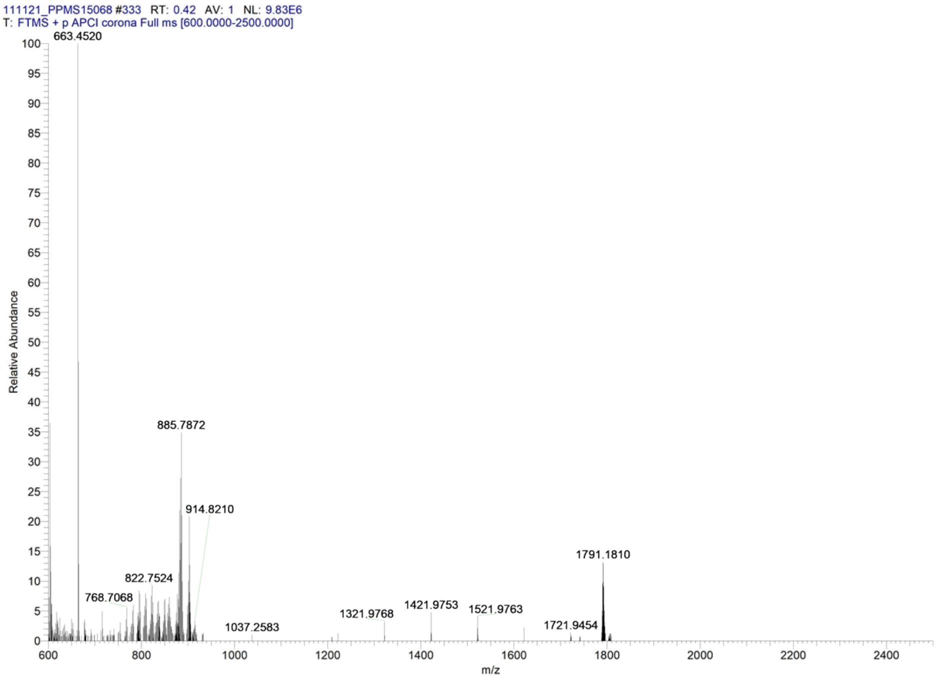

Figure S25. APCI-MS of 1,2-bis(5-(2-carbaldehyde-4,4,9,9-tetraoctyl-4,9-dihydro-*s*-indaceno[1,2-*b*:5,6-*b′*]dithiophen-7-yl)thiophen-2-yl)-*ortho*-carborane.

1,12-bis(5-((*Z*)-2-((1-(dicyanomethylene)-3-oxo-1,3-dihydro-2*H*-inden-2-ylidene)methyl)-4,4,9,9-tetraoctyl-4,9-dihydro-*s*-indaceno[1,2-*b*:5,6-*b′*]dithiophen-7-yl)thiophen-2-yl)-*para*-carborane:

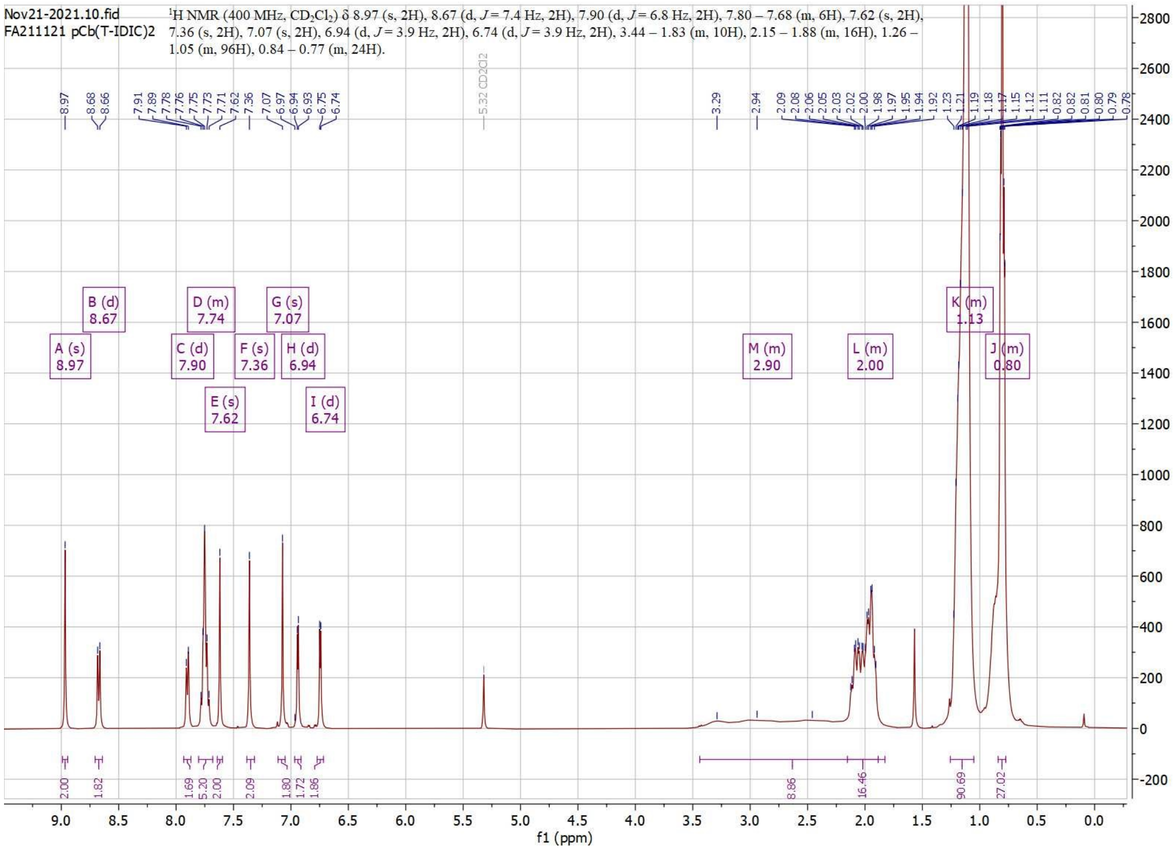

^{1}H NMR (400 MHz, CD_2Cl_2) δ 8.97 (s, 2H), 8.67 (d, *J* = 7.4 Hz, 2H), 7.90 (d, *J* = 6.8 Hz, 2H), 7.80 – 7.68 (m, 6H), 7.62 (s, 2H), 7.36 (s, 2H), 7.07 (s, 2H), 6.94 (d, *J* = 3.9 Hz, 2H), 6.74 (d, *J* = 3.9 Hz, 2H), 3.44 – 1.83 (m, 10H), 2.15 – 1.88 (m, 16H), 1.26 – 1.05 (m, 96H), 0.84 – 0.77 (m, 24H).

Figure S26. ^{1}H NMR spectrum of 1,12-bis(5-((*Z*)-2-((1-(dicyanomethylene)-3-oxo-1,3-dihydro-2*H*-inden-2-ylidene)methyl)-4,4,9,9-tetraoctyl-4,9-dihydro-*s*-indaceno[1,2-*b*:5,6-*b′*]dithiophen-7-yl)thiophen-2-yl)-*para*-carborane.

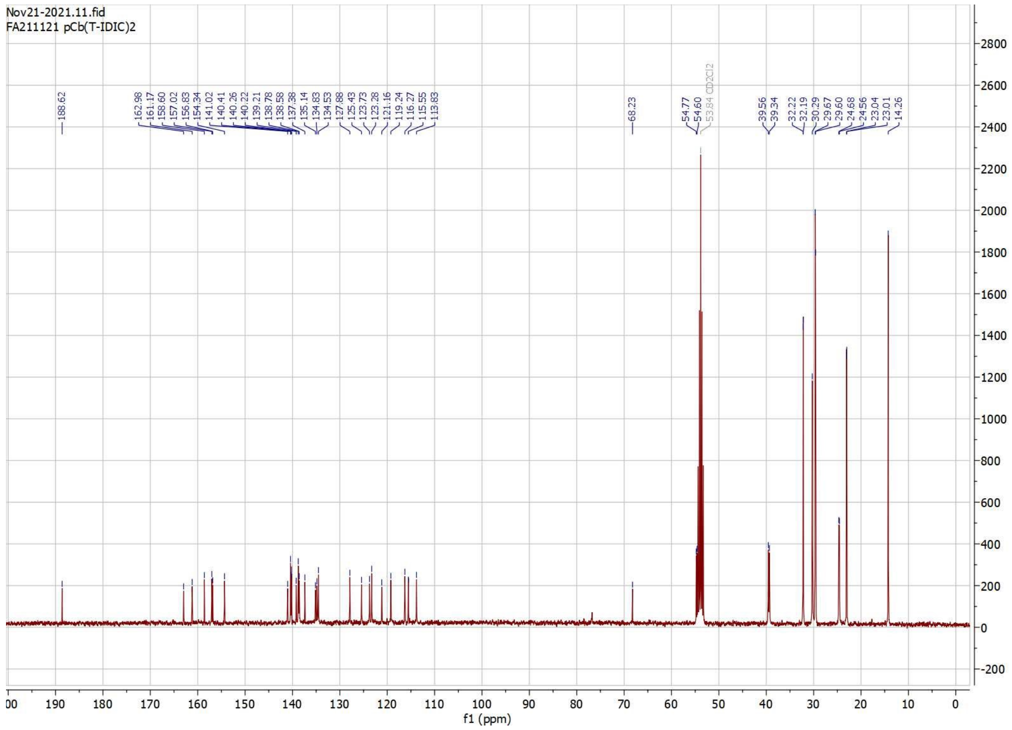

Figure S27. ^{13}C NMR spectrum of 1,12-bis(5-((*Z*)-2-((1-(dicyanomethylene)-3-oxo-1,3-dihydro-2*H*-inden-2-ylidene)methyl)-4,4,9,9-tetraoctyl-4,9-dihydro-*s*-indaceno[1,2-*b*:5,6-*b'*]dithiophen-7-yl)thiophen-2-yl)-*para*-carborane.

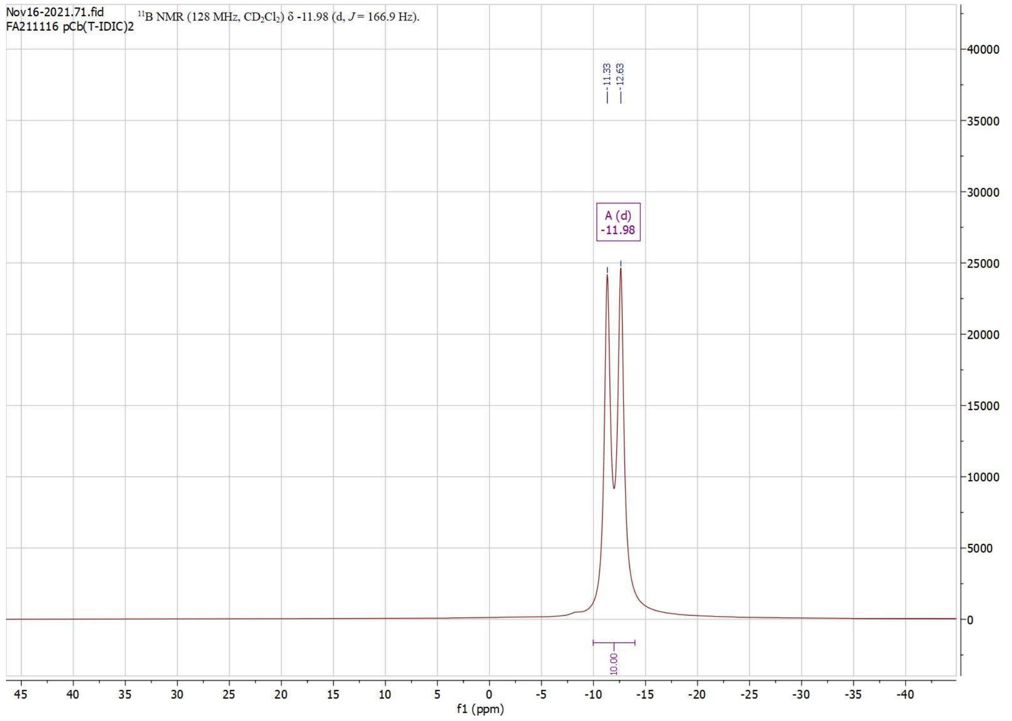

Figure S28. ^{11}B NMR spectrum of 1,12-bis(5-((*Z*)-2-((1-(dicyanomethylene)-3-oxo-1,3-dihydro-2*H*-inden-2-ylidene)methyl)-4,4,9,9-tetraoctyl-4,9-dihydro-*s*-indaceno[1,2-*b*:5,6-*b'*]dithiophen-7-yl)thiophen-2-yl)-*para*-carborane.

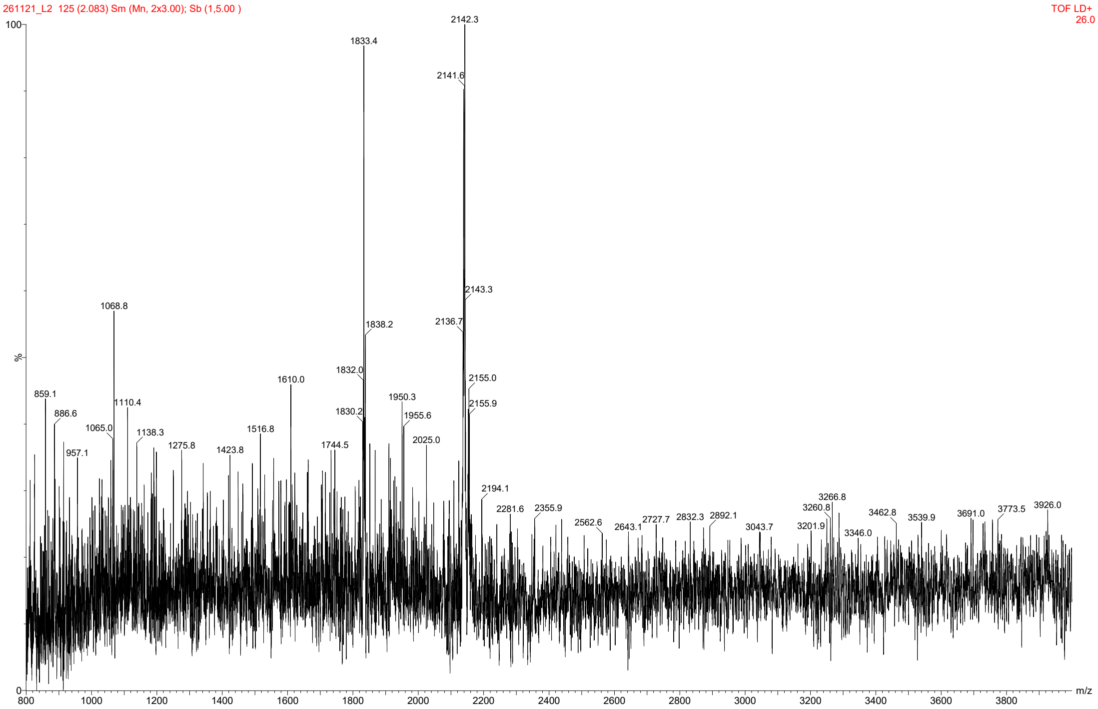

Figure S29. MALDI of 1,12-bis(5-((*Z*)-2-((1-(dicyanomethylene)-3-oxo-1,3-dihydro-2*H*-inden-2-ylidene)methyl)-4,4,9,9-tetraoctyl-4,9-dihydro-*s*-indaceno[1,2-*b*:5,6-*b'*]dithiophen-7-yl)thiophen-2-yl)-*para*-carborane.

1,7-bis(5-((*Z*)-2-((1-(dicyanomethylene)-3-oxo-1,3-dihydro-2*H*-inden-2-ylidene)methyl)-4,4,9,9-tetraoctyl-4,9-dihydro-*s*-indaceno[1,2-*b*:5,6-*b′*]dithiophen-7-yl)thiophen-2-yl)-*meta*-carborane:

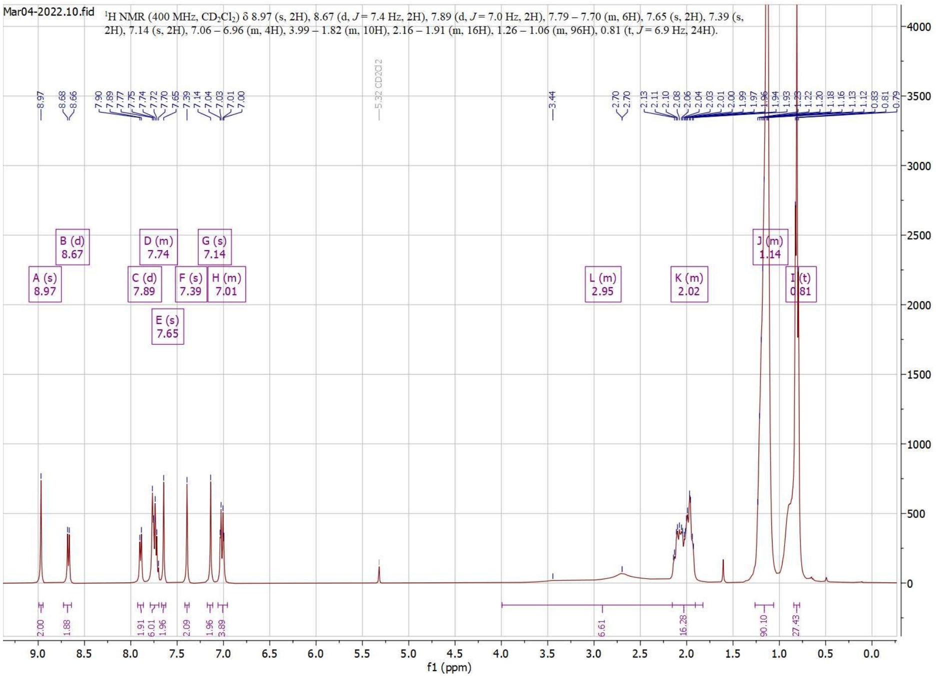

^{1}H NMR (400 MHz, CD_2Cl_2) δ 8.97 (s, 2H), 8.67 (d, *J* = 7.4 Hz, 2H), 7.89 (d, *J* = 7.0 Hz, 2H), 7.79 – 7.70 (m, 6H), 7.65 (s, 2H), 7.39 (s, 2H), 7.14 (s, 2H), 7.06 – 6.96 (m, 4H), 3.99 – 1.82 (m, 10H), 2.16 – 1.91 (m, 16H), 1.26 – 1.06 (m, 96H), 0.81 (t, *J* = 6.9 Hz, 24H).

Figure S30. ^{1}H NMR spectrum of 1,7-bis(5-((*Z*)-2-((1-(dicyanomethylene)-3-oxo-1,3-dihydro-2*H*-inden-2-ylidene)methyl)-4,4,9,9-tetraoctyl-4,9-dihydro-*s*-indaceno[1,2-*b*:5,6-*b′*]dithiophen-7-yl)thiophen-2-yl)-*meta*-carborane.

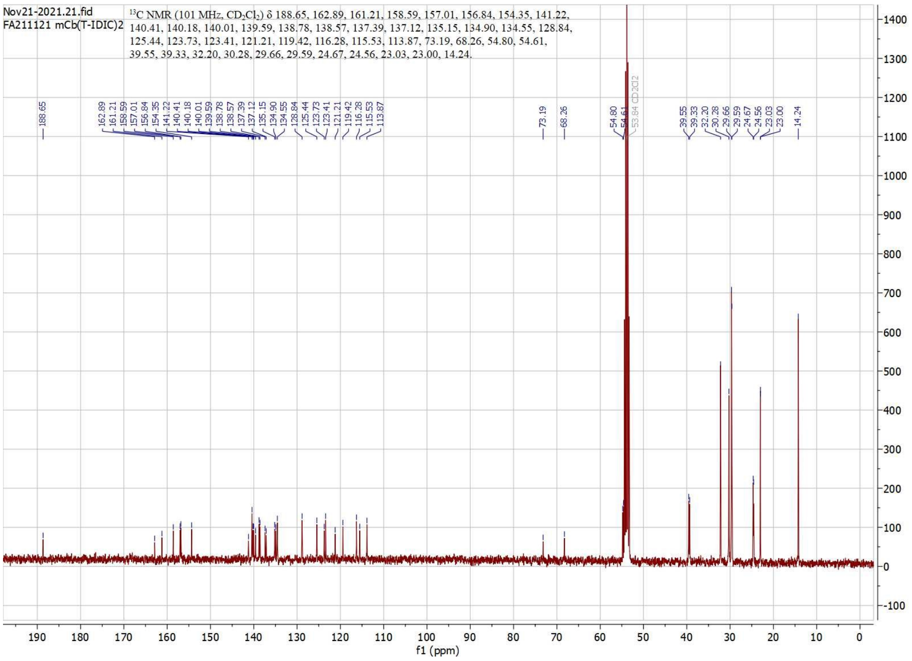

^{13}C NMR (101 MHz, CD_2Cl_2) δ 188.65, 162.89, 161.21, 158.59, 157.01, 156.84, 154.35, 141.22, 140.41, 140.18, 140.01, 139.59, 138.78, 138.57, 137.39, 137.12, 135.15, 134.90, 134.55, 128.84, 125.44, 123.73, 123.41, 121.21, 119.42, 116.28, 115.53, 113.87, 73.19, 68.26, 54.80, 54.61, 39.55, 39.33, 32.20, 30.28, 29.66, 29.59, 24.67, 24.56, 23.03, 23.00, 14.24.

Figure S31. ^{13}C NMR spectrum of 1,7-bis(5-((*Z*)-2-((1-(dicyanomethylene)-3-oxo-1,3-dihydro-2*H*-inden-2-ylidene)methyl)-4,4,9,9-tetraoctyl-4,9-dihydro-*s*-indaceno[1,2-*b*:5,6-*b′*]dithiophen-7-yl)thiophen-2-yl)-*meta*-carborane.

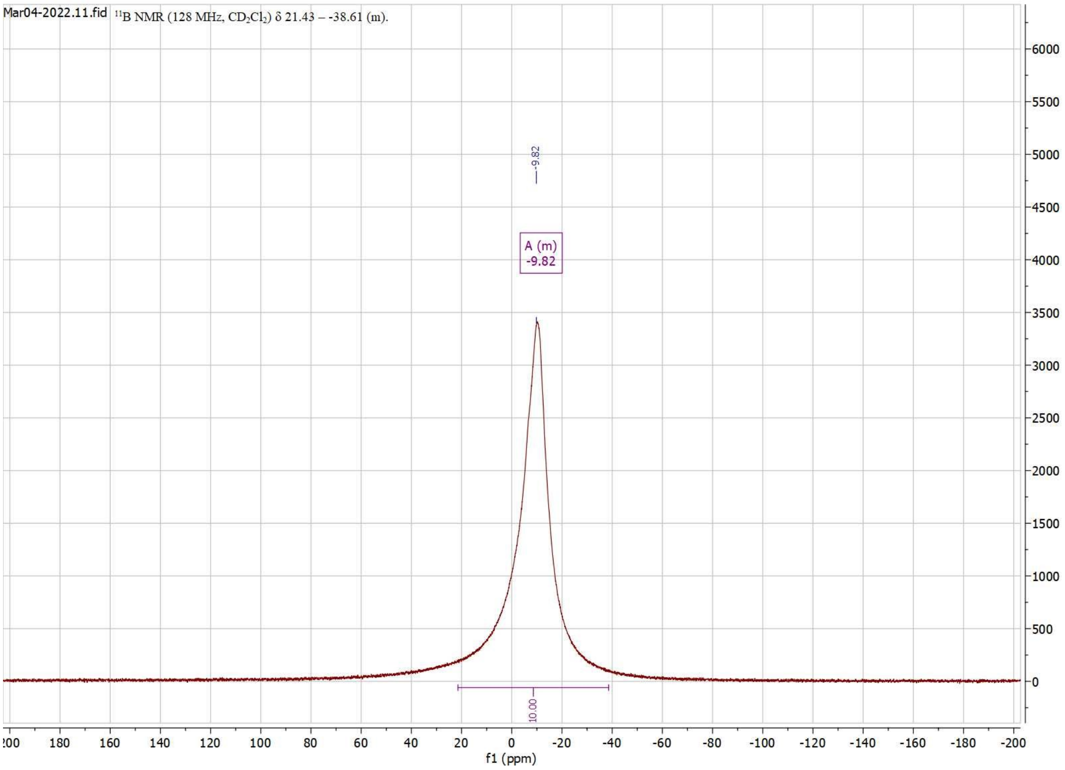

Figure S32. ^{11}B NMR spectrum of 1,7-bis(5-((*Z*)-2-((1-(dicyanomethylene)-3-oxo-1,3-dihydro-2*H*-inden-2-ylidene)methyl)-4,4,9,9-tetraoctyl-4,9-dihydro-*s*-indaceno[1,2-*b*:5,6-*b′*]dithiophen-7-yl)thiophen-2-yl)-*meta*-carborane.

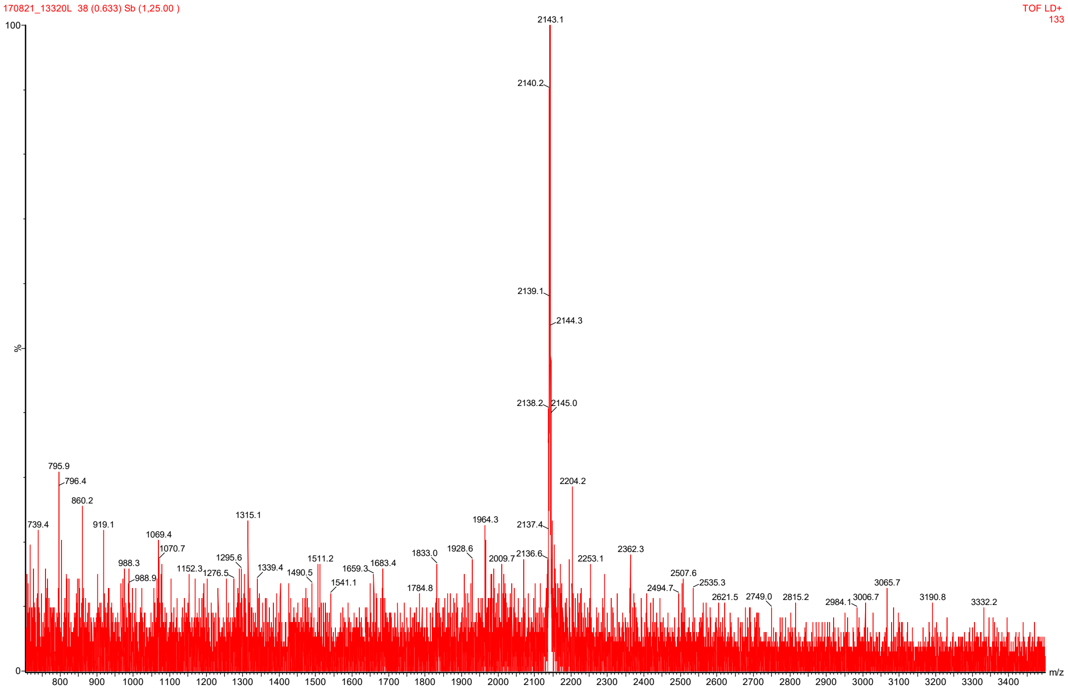

Figure S33. MALDI of 1,7-bis(5-((*Z*)-2-((1-(dicyanomethylene)-3-oxo-1,3-dihydro-2*H*-inden-2-ylidene)methyl)-4,4,9,9-tetraoctyl-4,9-dihydro-*s*-indaceno[1,2-*b*:5,6-*b′*]dithiophen-7-yl)thiophen-2-yl)-*meta*-carborane.

1,2-bis(5-((*Z*)-2-((1-(dicyanomethylene)- 3-oxo-1,3-dihydro-2*H*-inden-2-ylidene)methyl)-4,4,9,9-tetraoctyl-4,9-dihydro-*s*-indaceno[1,2-*b*:5,6-*b'*]dithiophen-7-yl)thiophen-2-yl)-*ortho*-carborane:

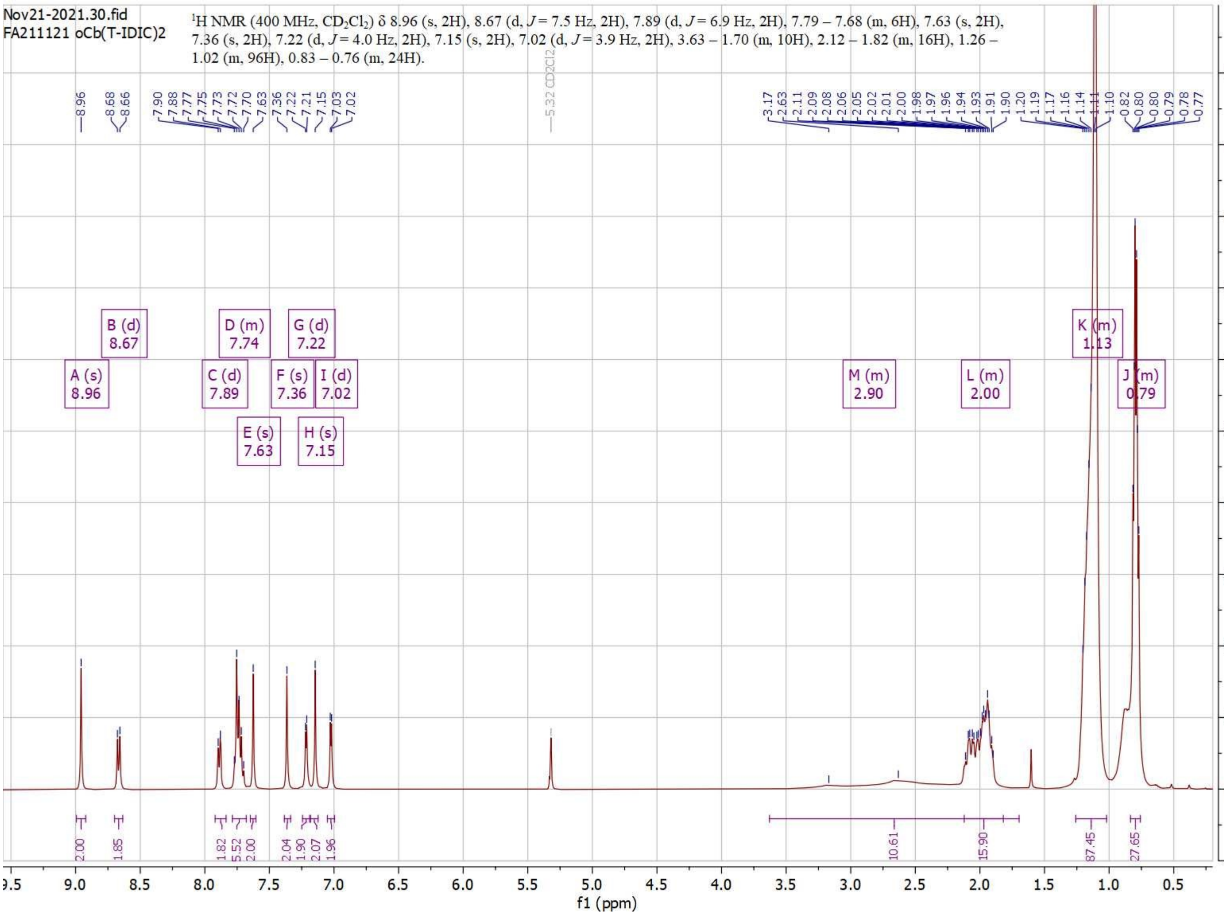

^{1}H NMR (400 MHz, CD_2Cl_2) δ 8.96 (s, 2H), 8.67 (d, *J* = 7.5 Hz, 2H), 7.89 (d, *J* = 6.9 Hz, 2H), 7.79 – 7.68 (m, 6H), 7.63 (s, 2H), 7.36 (s, 2H), 7.22 (d, *J* = 4.0 Hz, 2H), 7.15 (s, 2H), 7.02 (d, *J* = 3.9 Hz, 2H), 3.63 – 1.70 (m, 10H), 2.12 – 1.82 (m, 16H), 1.26 – 1.02 (m, 96H), 0.83 – 0.76 (m, 24H).

Figure S34. ^{1}H NMR spectrum of 1,2-bis(5-((*Z*)-2-((1-(dicyanomethylene)- 3-oxo-1,3-dihydro-2*H*-inden-2-ylidene)methyl)-4,4,9,9-tetraoctyl-4,9-dihydro-*s*-indaceno[1,2-*b*:5,6-*b'*]dithiophen-7-yl)thiophen-2-yl)-*ortho*-carborane.

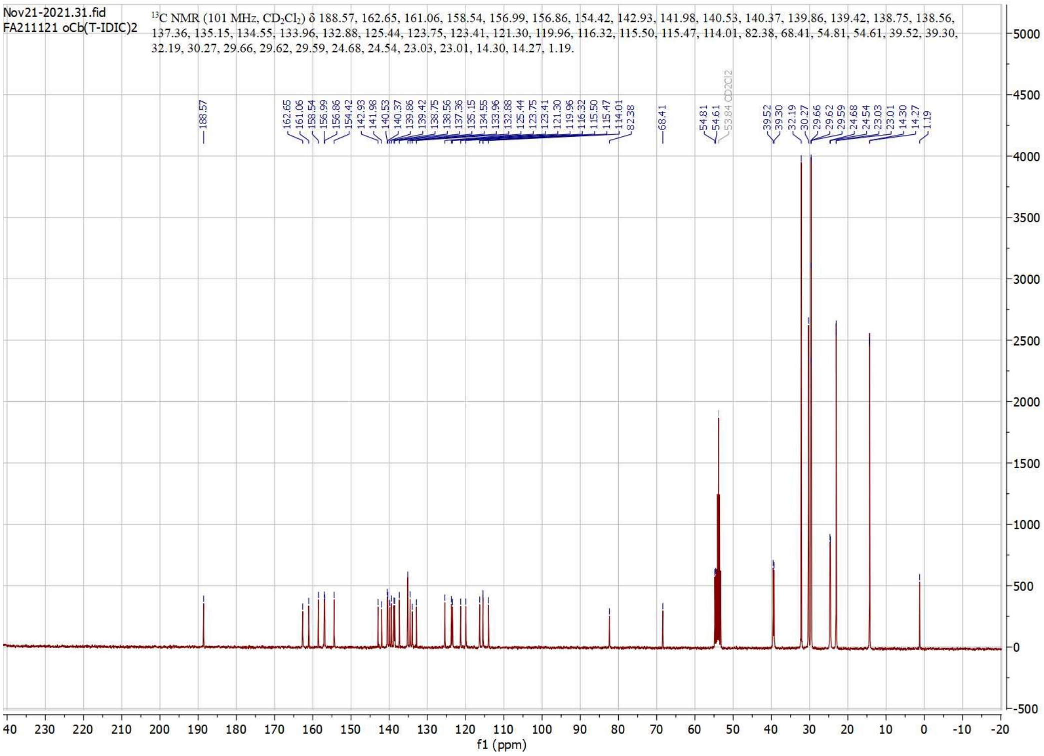

^{13}C NMR (101 MHz, CD_2Cl_2) δ 188.57, 162.65, 161.06, 158.54, 156.99, 156.86, 154.42, 142.93, 141.98, 140.53, 140.37, 139.86, 139.42, 138.75, 138.56, 137.36, 135.15, 134.55, 133.96, 132.88, 125.44, 123.75, 123.41, 121.30, 119.96, 116.32, 115.50, 115.47, 114.01, 82.38, 68.41, 54.81, 54.61, 39.52, 39.30, 32.19, 30.27, 29.66, 29.62, 29.59, 24.68, 24.54, 23.03, 23.01, 14.30, 14.27, 1.19.

Figure S35. ^{13}C NMR spectrum of 1,2-bis(5-((*Z*)-2-((1-(dicyanomethylene)-3-oxo-1,3-dihydro-2*H*-inden-2-ylidene)methyl)-4,4,9,9-tetraoctyl-4,9-dihydro-*s*-indaceno[1,2-*b*:5,6-*b'*]dithiophen-7-yl)thiophen-2-yl)-*ortho*-carborane.

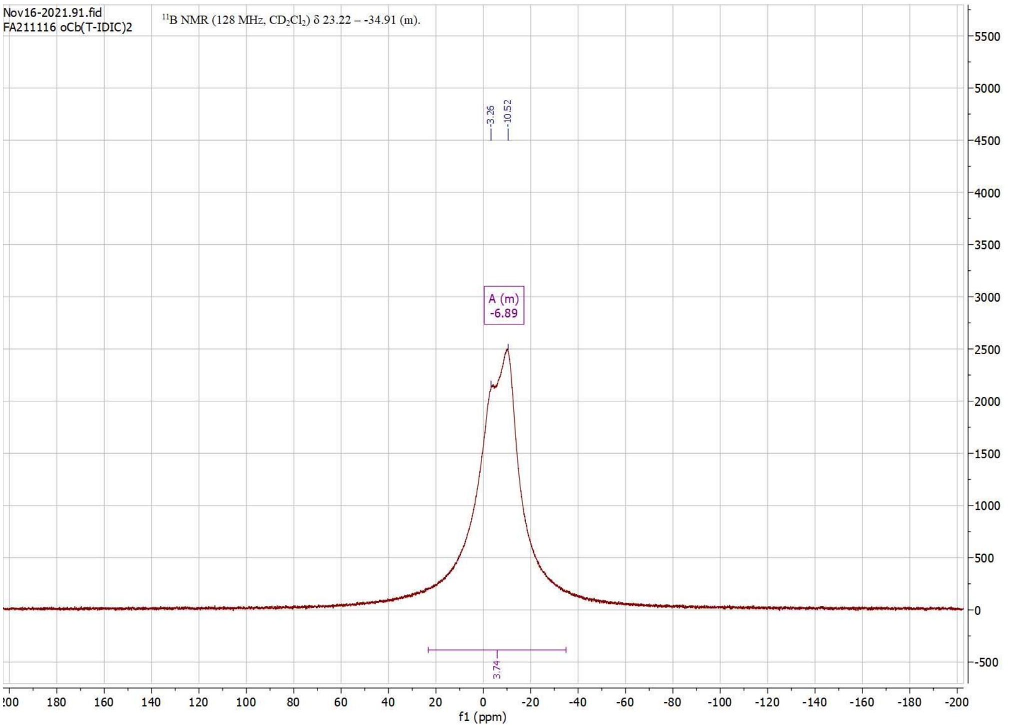

^{11}B NMR (128 MHz, CD_2Cl_2) δ 23.22 – -34.91 (m).

Figure S36. ^{11}B NMR spectrum of 1,2-bis(5-((*Z*)-2-((1-(dicyanomethylene)- 3-oxo-1,3-dihydro-2*H*-inden-2-ylidene)methyl)-4,4,9,9-tetraoctyl-4,9-dihydro-*s*-indaceno[1,2-*b*:5,6-*b'*]dithiophen-7-yl)thiophen-2-yl)-*ortho*-carborane.

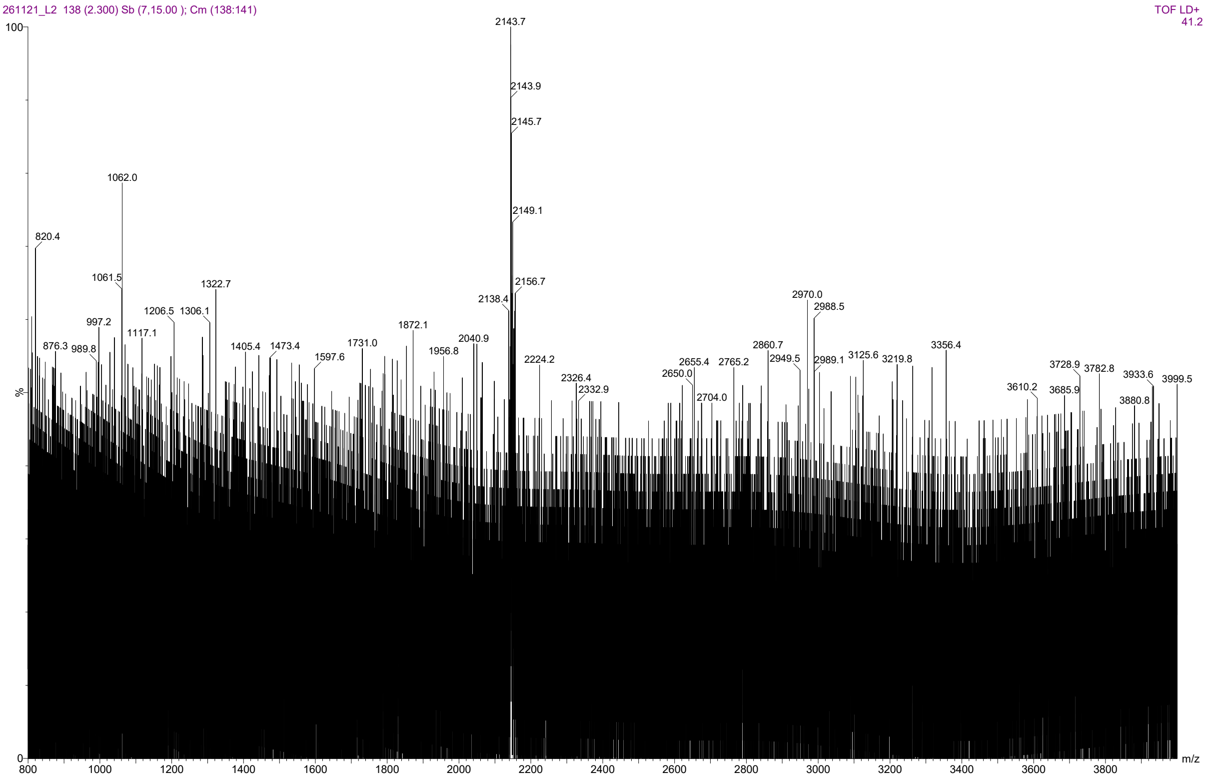

Figure S37. MALDI of 1,2-bis(5-((*Z*)-2-((1-(dicyanomethylene)-3-oxo-1,3-dihydro-2*H*-inden-2-ylidene)methyl)-4,4,9,9-tetraoctyl-4,9-dihydro-*s*-indaceno[1,2-*b*:5,6-*b'*]dithiophen-7-yl)thiophen-2-yl)-*ortho*-carborane.

1,2-bis(5-((*Z*)-2-((1-(dicyanomethylene)-5,6-difluoro-3-oxo-1,3-dihydro-2*H*-inden-2-ylidene)methyl)-4,4,9,9-tetraoctyl-4,9-dihydro-*s*-indaceno[1,2-*b*:5,6-*b'*]dithiophen-7-yl)thiophen-2-yl)-*ortho*-carborane:

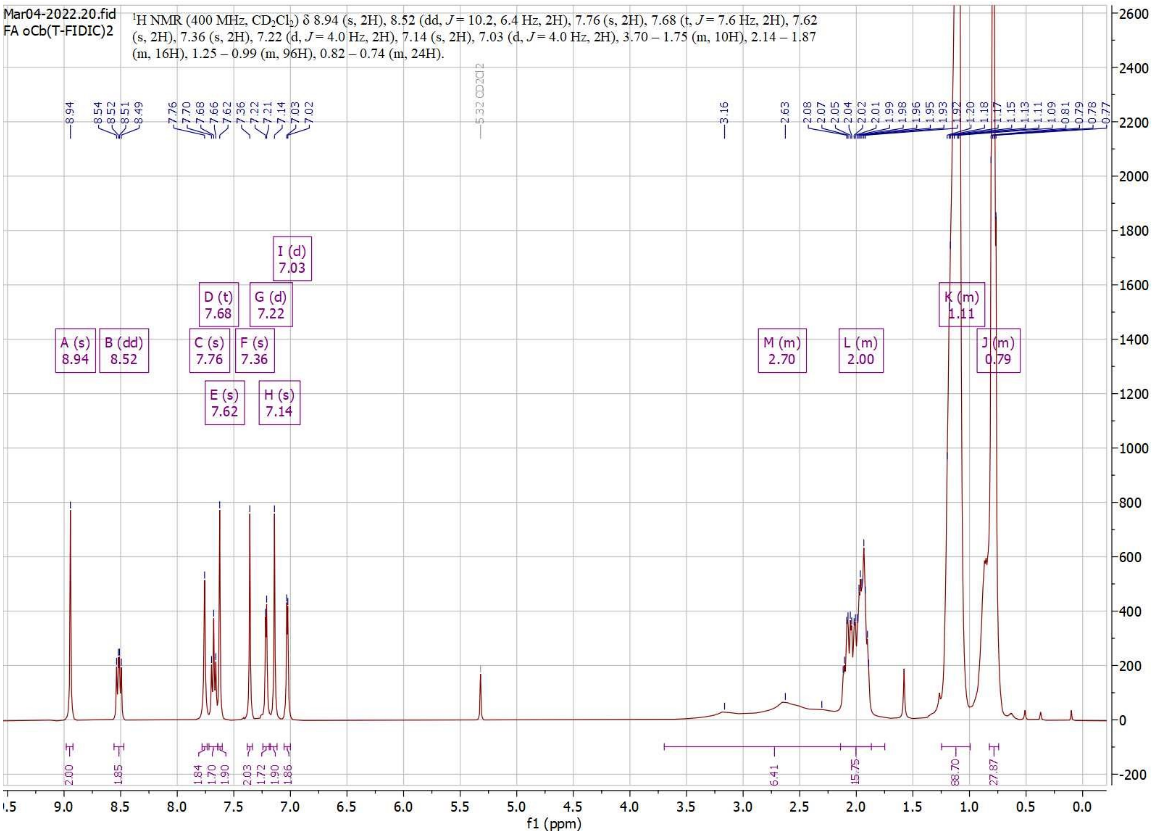

^{1}H NMR (400 MHz, CD_2Cl_2) δ 8.94 (s, 2H), 8.52 (dd, *J* = 10.2, 6.4 Hz, 2H), 7.76 (s, 2H), 7.68 (t, *J* = 7.6 Hz, 2H), 7.62 (s, 2H), 7.36 (s, 2H), 7.22 (d, *J* = 4.0 Hz, 2H), 7.14 (s, 2H), 7.03 (d, *J* = 4.0 Hz, 2H), 3.70 – 1.75 (m, 10H), 2.14 – 1.87 (m, 16H), 1.25 – 0.99 (m, 96H), 0.82 – 0.74 (m, 24H).

Figure S38. ^{1}H NMR spectrum of 1,2-bis(5-((*Z*)-2-((1-(dicyanomethylene)-5,6-difluoro-3-oxo-1,3-dihydro-2*H*-inden-2-ylidene)methyl)-4,4,9,9-tetraoctyl-4,9-dihydro-*s*-indaceno[1,2-*b*:5,6-*b'*]dithiophen-7-yl)thiophen-2-yl)-*ortho*-carborane.

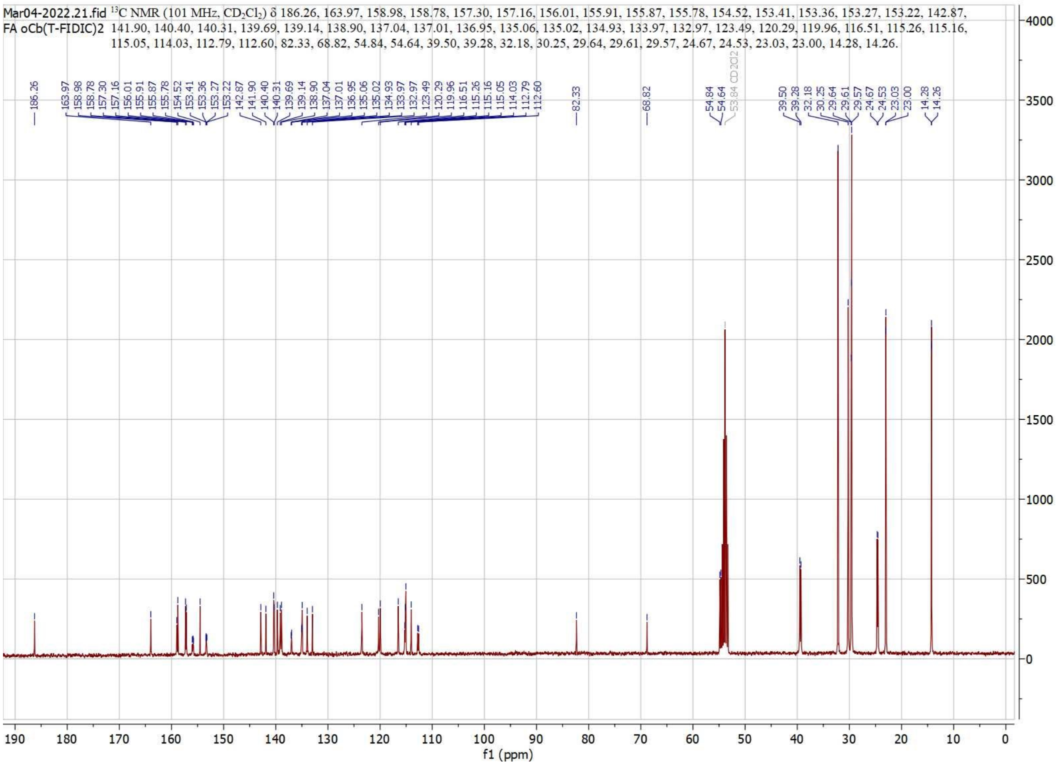

Figure S39. ^{13}C NMR spectrum of 1,2-bis(5-((*Z*)-2-((1-(dicyanomethylene)-5,6-difluoro-3-oxo-1,3-dihydro-2*H*-inden-2-ylidene)methyl)-4,4,9,9-tetraoctyl-4,9-dihydro-*s*-indaceno[1,2-*b*:5,6-*b'*]dithiophen-7-yl)thiophen-2-yl)-*ortho*-carborane.

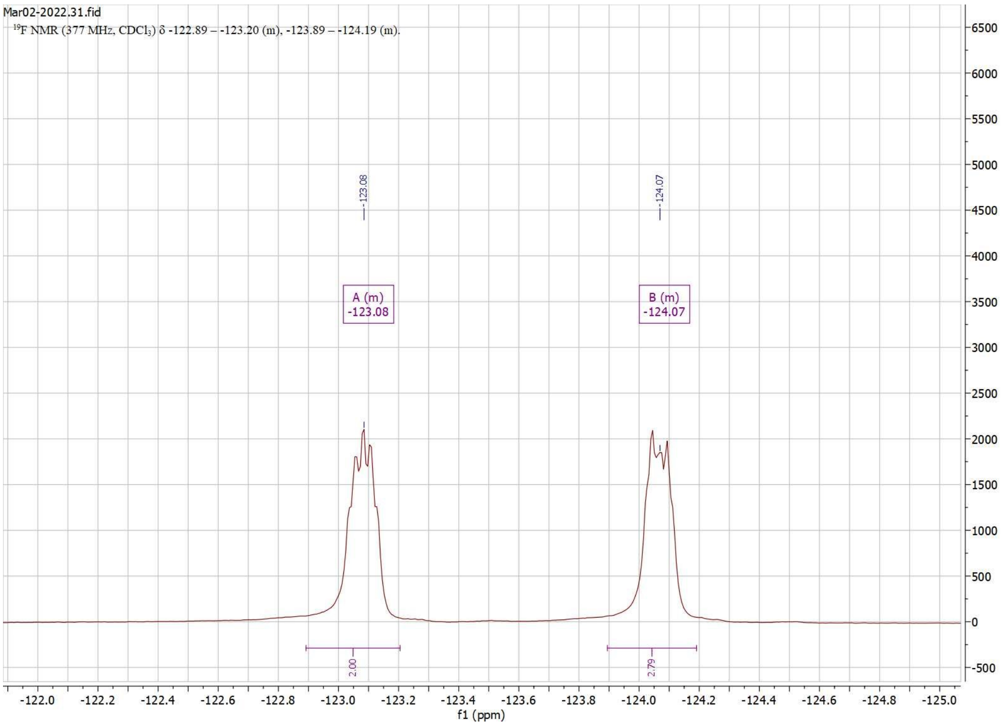

Figure S40. ^{19}F NMR spectrum of 1,2-bis(5-((*Z*)-2-((1-(dicyanomethylene)-5,6-difluoro-3-oxo-1,3-dihydro-2*H*-inden-2-ylidene)methyl)-4,4,9,9-tetraoctyl-4,9-dihydro-*s*-indaceno[1,2-*b*:5,6-*b'*]dithiophen-7-yl)thiophen-2-yl)-*ortho*-carborane.

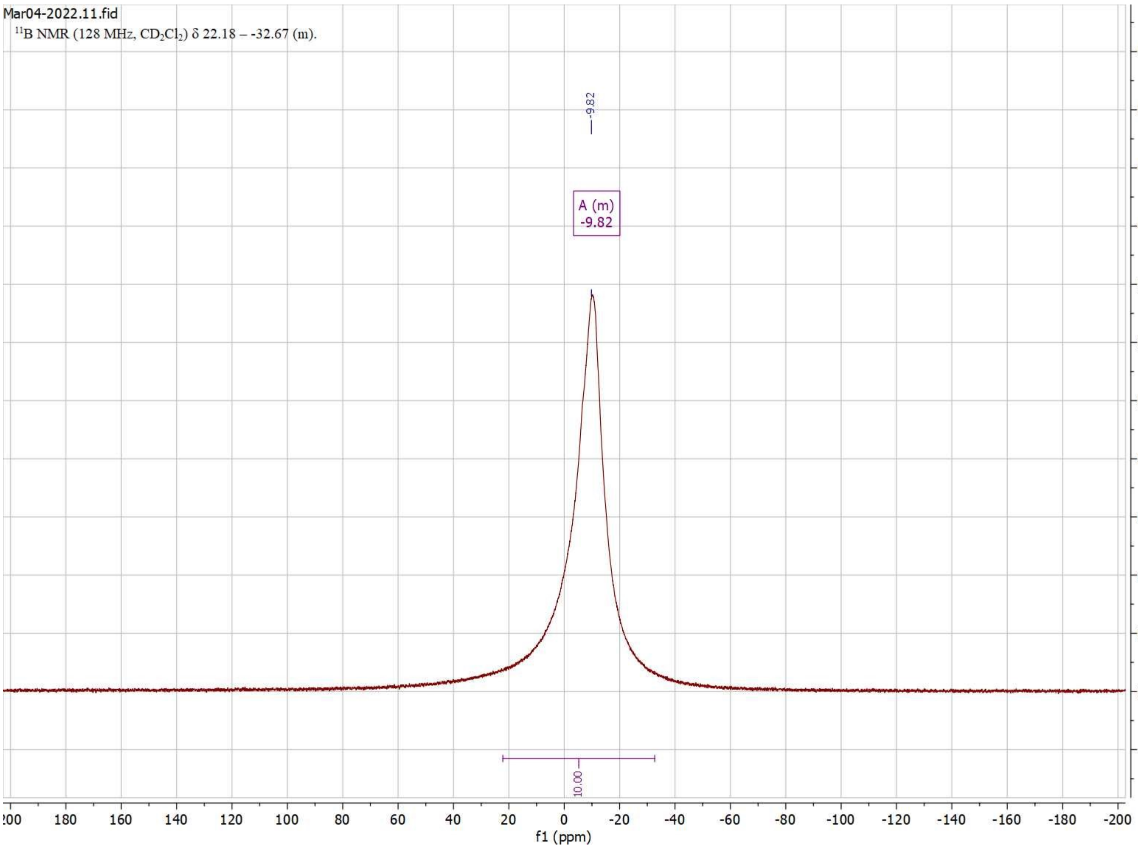

Figure S41. ^{11}B NMR spectrum of 1,2-bis(5-((*Z*)-2-((1-(dicyanomethylene)-5,6-difluoro-3-oxo-1,3-dihydro-2*H*-inden-2-ylidene)methyl)-4,4,9,9-tetraoctyl-4,9-dihydro-*s*-indaceno[1,2-*b*:5,6-*b'*]dithiophen-7-yl)thiophen-2-yl)-*ortho*-carborane.

References

[S1] Gaussian 16, Revision C.01, M.J. Frisch, G.W. Trucks, H.B. Schlegel, G.E. Scuseria, M.A. Robb, J.R. Cheeseman, G. Scalmani, V. Barone, G.A. Petersson, H. Nakatsuji, X. Li, M. Caricato, A. v. Marenich, J. Bloino, B.G. Janesko, R. Gomperts, B. Mennucci, H.P. Hratchian, J. v. Ortiz, A.F. Izmaylov, J.L. Sonnenberg, D. Williams-Young, F. Ding, F. Lipparini, F. Egidi, J. Goings, B. Peng, A. Petrone, T. Henderson, D. Ranasinghe, V.G. Zakrzewski, J. Gao, N. Rega, G. Zheng, W. Liang, M. Hada, M. Ehara, K. Toyota, R. Fukuda, J. Hasegawa, M. Ishida, T. Nakajima, Y. Honda, O. Kitao, H. Nakai, T. Vreven, K. Throssell, J.A., Jr. Montgomery, J.E. Peralta, F. Ogliaro, M.J. Bearpark, J.J. Heyd, E.N. Brothers, K.N. Kudin, V.N. Staroverov, T.A. Keith, R. Kobayashi, J. Normand, K. Raghavachari, A.P. Rendell, J.C. Burant, S.S. Iyengar, J. Tomasi, M. Cossi, J.M. Millam, M. Klene, C. Adamo, R. Cammi, J.W. Ochterski, R.L. Martin, K. Morokuma, O. Farkas, J.B. Foresman, D.J. Fox. Gaussian Inc., Wallingford CT, 2016.

[S2] A.D. Becke, Density-functional thermochemistry. III. The role of exact exchange, The Journal of Chemical Physics. 98 (1993) 5648–5652. https://doi.org/10.1063/1.464913.